# Insights into the petrogenesis of lunar basaltic breccia Dominion Range (DOM) 18543

**Alex Schweitzer[1], Claire L. McLeod[1]*, Aleksandra J. Gawronska[2,3], Azadeh Sedaghat[1], Marion L. Lytle[1], Barry Shaulis[4] and Matthew Loocke[5]**

[1]Department of Geology and Environmental Earth Science, Miami University, Oxford, Ohio 45056, USA

[2]Department of Physics, Catholic University of America, Washington, DC 20064, USA

[3]NASA Goddard Space Flight Center, Greenbelt, MD 20771, USA

[4]Trace Element and Radiogenic Isotope Laboratory (TRAIL), University of Arkansas, Fayetteville, AR 72701, USA

[5]Department of Geology and Geophysics, Louisiana State University, Baton Rouge, LA 70803, USA

CLM, 0000-0001-8212-2287; AJG, 0000-0002-3470-1177; AS, 0009-0009-0489-5351; MLL, 0000-0002-7214-4850; BS, 0000-0003-0707-8137; ML, 0000-0001-7660-2516
*Correspondence: mcleodcl@miamioh.edu

**Abstract:** From the 2018–19 Antarctic Search for Meteorites (ANSMET) season, eight polymict, basaltic lunar regolith breccias were recovered from the Dominion Range (DOM). This study examines DOM 18543,9, a clast-poor breccia (<10%) containing clasts of basalts, gabbros, impact melt breccias, three-phase symplectites and one microbreccia containing a Ferroan Anorthosite (FAN)-derived, anorthositic granulite. All clasts and mineral fragments are set in a glassy matrix that contains glassy melt veins, pockets and impact glass spherules. Pyroxene and olivine Fe/Mn systematics are consistent with a lunar origin. Pyroxenes are augites and pigeonites, olivines are predominantly fayalitic ($Fa_{85–99}$) and plagioclase is typically anorthitic ($An_{93–99}$). Pyroxene, ilmenite and olivine compositions are consistent with derivation from a compositionally evolved, low-Ti basaltic magma and represent the relatively late stages of fractionation. Textural and geochemical characteristics are similar to those of the YAMM group, indicating a potential shared source from an ancient, low-Ti, KREEP (potassium, rare-earth elements and phosphorus)-poor lava flow in a mare terrane where feldspathic material is locally available. While some characteristics are shared with an unnamed crater within the Schickard crater, characterization of paired meteorites within the DOM clan, alongside cosmic ray exposure dating and integration of remote-sensing observations, is required to refine the petrological framework of these recently discovered lunar samples.

**Supplementary material:** Tables and additional datasets providing insights into the petrogenesis of lunar basaltic breccia DOM 18543 are available at https://doi.org/10.6084/m9.figshare.c.8293723

Understanding the processes and timescales over which the rocky objects of the Solar System formed has relied on a wide variety of scientific approaches: observations via telescopes, crewed landings, sample return and remote sensing via satellites (e.g. Taylor 1994; Des Marais *et al.* 2004; Chauhan *et al.* 2015; Baars and Kärcher 2018; Jolliff and Robinson 2019; Pernet-Fisher *et al.* 2019; Cambioni *et al.* 2021; Slyuta 2021; Wiedner *et al.* 2021; Li *et al.* 2022; Kim *et al.* 2023; Sánchez-Lavega *et al.* 2023; Sheng *et al.* 2025). This integrated, multidisciplinary approach has significantly expanded our understanding of rocky body formative processes, the timescales over which differentiated rocky objects evolve, and the geological processes which characterize an object's geological history in the absence of a mobile lid plate tectonic regime and an active hydrological cycle (e.g. Basilevsky and Head 1998; Hauck *et al.* 2004; Breuer *et al.* 2007; Bouvier *et al.* 2009; Carr and Head 2010; Hiesinger *et al.* 2016; McSween *et al.* 2019; Udry *et al.* 2020, 2025; Tosi and Padovan 2021; Zhou *et al.* 2022; Ghail *et al.* 2024; S. Li *et al.* 2024).

The Moon is Earth's nearest neighbour in space and was first mentioned as being rocky in nature by the 5th century Greek philosopher Anaxagoras of Clazomenae who described the dark patches as 'an uneven "earthy" layer' (Bicknell 1969). At present, it is the most extensively sampled differentiated planetary object. Human and robotic sample return

From: Mitchell, J. T., Barrett, T. J., King, A. J. and Stephen, N. R. (eds) *A Tour of the Solid Solar System: Recognizing Early Career Contributions to Extraterrestrial Geology*. Geological Society, London, Special Publications, **562**, https://doi.org/10.1144/gslspecpub2025-65

(i.e. Apollo, Luna and Chang'e), and the delivery of lunar meteorites via bombardment and ejection, have yielded the most diverse suite of sample types and lithologies from any known rocky body: soils, agglutinates, glass beads, and rocks including basalts, anorthosites, the Mg-suite, the alkali suite and a wide variety of breccias (e.g. Wood *et al.* 1970; Papike *et al.* 1976; Shearer and Papike 1993; Norman 2005; Slyuta 2014; Shearer *et al.* 2015; Du and Yang 2024; Zhang *et al.* 2025).

While materials returned from sample return missions are spatially constrained (Apollo, Luna, Chang'e), these represent a relatively limited sampling of the lunar surface: approximately 5% (Eugster 1989; Warren *et al.* 1989; Heiken *et al.* 1991; Harvey 2003; Atkinson 2010). The study of lunar meteorites therefore has the potential to expand and advance our understanding of the Moon's geological history beyond those regions targeted by surface missions as they represent a random sampling of the lunar surface (Korotev 2005). As of December 2024, 1541 kg of lunar samples are known to exist on Earth, of which 382 kg (NASA 2023) of materials are associated with returned samples from the lunar surface (25% of the total lunar material). Most recently, Chang'e 5 and 6 returned ~3.7 kg of materials including the first set of samples from the lunar farside (Joy *et al.* 2025). The remaining 1159 kg (75%) of samples are associated with lunar meteorites which collectively represent <2% of all stony meteorites (Righter *et al.* 2023; Korotev 2025*a*,*b*).

Within the context of the lunar meteorite collection, <10% have been recovered from Antarctica and their average mass is low at ~26 g ($n = 44$), compared to 47 g from the Arabian Peninsula ($n = 75$) and 281 g ($n = 461$) from Northern Africa (Korotev 2025*a*,*b*), although the collective mass of Antarctic lunar meteorites is still more than five times that of the rocks (>1 cm) returned by the Apollo missions (see Fig. 1a; Korotev 2025*a*,*b*). The 2018–19 Antarctic Search for Meteorites (ANSMET) recovered the Dominion Range (DOM) 18242 clan weighing a total of 140.85 g (Righter *et al.* 2023; Righter 2024). Initially reported across three ANSMET newsletters, a total of eight stones are associated with this clan: 18242, 18244, 18262, 18509, 18543, 18545, 18666 and 18678 (Fig. 1b; Satterwhite and Righter 2019, 2020, 2022). From Righter *et al.* (2023), all of these samples 'were found near the northern edge of the blue ice tongue or at the edge in the moraine, p2' (Fig. 1b). In this contribution, the first detailed and integrated textural, mineralogical and geochemical characteristics of one of these 2018–19 DOM lunar meteorites, DOM 18543, are presented (Fig. 2a–c). Specifically, split 9 forms the basis of this study (Fig. 2d, e). The thin section was investigated via light microscopy, scanning electron microscopy (SEM), energy dispersive spectroscopy (EDS) and electron microprobe analysis (EPMA). Data were used to evaluate breccia petrogenesis and to place the origin of DOM 18543 within the context of the existing lunar geological framework.

## The 2018–19 Dominion Range (DOM) lunar meteorites

From the Meteoritical Bulletin Database (see also Table S1, Gattacceca *et al.* 2020), K. Pando, C. Corrigan and T. McCoy summarized initial textural, mineralogical and geochemical observations for the 2018–19 lunar DOM suite on the basis of DOM 18242 with Corrigan and McCoy noting that, within the context of all samples within the clan, 'sections are similar enough that one description will suffice'. These meteorites are highly brecciated basaltic breccias, specifically polymict regolith breccias with exteriors characterized by a black to dark grey fusion crust with occasional white speckles up to 1 mm in size and minor oxidation across most of the surface. Fresh sample surfaces are characterized by a black glassy matrix containing an assemblage of individual mineral fragments up to 0.5 mm in size, consisting largely of anorthitic plagioclase ($An_{91–99}$), pyroxenes of augite and pigeonite composition ($Fs_{20–64}$, $En_{16–41}$,$Wo_{20–39}$), with rarer orthopyroxenes ($Fs_{30}$-$En_{67}Wo_3$; Gattacceca *et al.* 2020). Also noted as being present were gabbro and symplectite clasts in addition to melt veins and melt pockets with the presence of a fine-grained 'anorthositic fragment' in DOM 18242 (Gattacceca *et al.* 2020). Accessory minerals present within the DOM suite were first reported for samples DOM 18262 and 18666 and included apatite, ilmenite, merrilite, troilite, zircon, $SiO_2$ polymorphs and occasional potassium feldspar (Gross *et al.* 2020; Zeigler *et al.* 2021; Hayden *et al.* 2022*a*, *b*; Hayden 2023).

Additional petrographic and geochemical studies of DOM 18262, 18509, 18543, 18666 and 18678 are reported in: Gross *et al.* (2020), McLeod *et al.* (2020), Zeigler *et al.* (2021), Hayden *et al.* (2021, 2022*a*, *b*), Schweitzer *et al.* (2022*a*,*b*), Gugino *et al.* (2024*a*, *b*), McLeod *et al.* (2024), and McLeod and Sedaghat (2025). Collectively, these studies report the presence of several lithic clasts including gabbro, basalt, anorthosite, impact melt breccias and symplectites. Clasts are somewhat rare, accounting for <5% of the total composition. Rarer quartz monzodiorites (QMDs) and felsites were also reported in Hayden *et al.* (2022*a*, *b*) and Hayden (2023). Mineral fragments vary in size from <10 μm in the brecciated, glassy matrix up to a few millimetres in length. Minerals are predominantly plagioclase and pyroxenes, with occasional olivines, opaque oxides and silica-rich minerals. Additionally, individual mineral

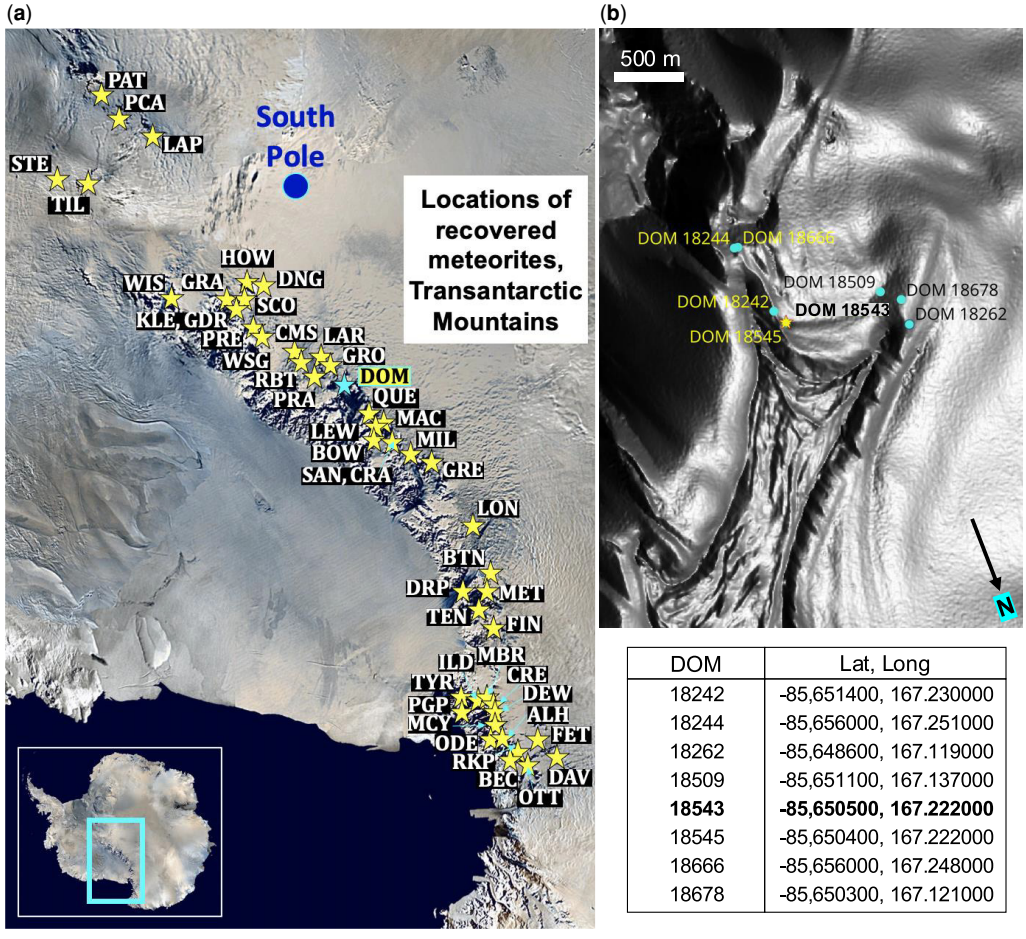


| DOM | Lat, Long |
|---|---|
| 18242 | -85,651400, 167.230000 |
| 18244 | -85,656000, 167.251000 |
| 18262 | -85,648600, 167.119000 |
| 18509 | -85,651100, 167.137000 |
| **18543** | **-85,650500, 167.222000** |
| 18545 | -85,650400, 167.222000 |
| 18666 | -85,656000, 167.248000 |
| 18678 | -85,650300, 167.121000 |

**Fig. 1.** (**a**) Map summarizing the locations from which meteorites have been returned through the Antarctic Search for Meteorites (ANSMET) programme, with the Dominion (DOM) Range shown by the blue star. (**b**) Locations of the 2018–19 lunar DOM meteorites. Meteorite locations (and .kml files) are available in the Meteoritical Bulletin Database. The 2018–19 lunar DOM meteorites were reported in three *Antarctic Meteorite Newsletters* (Satterwhite and Righter 2019, 2020, 2022). DOM 18543 was reported in Satterwhite and Righter (2019). Lunar meteorite DOM 18543 (yellow star) is the focus of this study. See also Righter *et al.* (2023) and Righter (2024). Source: (a) map modified from NASA; (b) basemap provided by the Reference Elevation Model of Antarctica (REMA) accessed via https://rema.apps.pgc.umn.edu/ (Howat *et al.* 2019; Polar Geospatial Center 2019).

fragments, symplectites, and melt veins, pockets and spherules are common. Mineral chemical analyses classify plagioclase as anorthitic ($An_{82–97}$,$Ab_{3–18}$, $Or_{0.1–0.5}$) and pyroxenes as Fe-rich pigeonites and augites ($Fs_{26–98}$,$En_{1–68}$,$Wo_{1–42}$) with some exhibiting exsolution lamellae. Olivines in DOM 18509, 18543, 18666 and 18678 are dominantly fayalitic ($Fa_{48–99}$,$Fo_{1–51}$). Hayden *et al.* (2022*a*, *b*) and Hayden (2023) also documented minor apatite and merrillite in DOM 18262 and 18666, from which $^{207}Pb/^{206}Pb$ ages were interpreted as crystallization ages between 3.86 and 3.96 Ga. Finally, Zeigler *et al.* (2021) analysed the major element composition of the fusion crust from samples DOM 18509, 18543 and 18678. This was used as a proxy for the bulk composition of the meteorite suites (Mg# (Mg/(Mg+Fe)): 23–24; $TiO_2$: 1.4–1.8 wt%; Zeigler *et al.* 2021). All analyses were within error of each other and it was inferred that they were paired. For further discussion on meteorite pairing relationships, see discussion later.

To better understand the petrological evolution of the 2018–19 lunar DOM clan, and to place this within the context of magmatic and brecciation processes on the Moon, this study focuses on DOM 18543 (Fig. 2a–c), specifically thin section split −9.

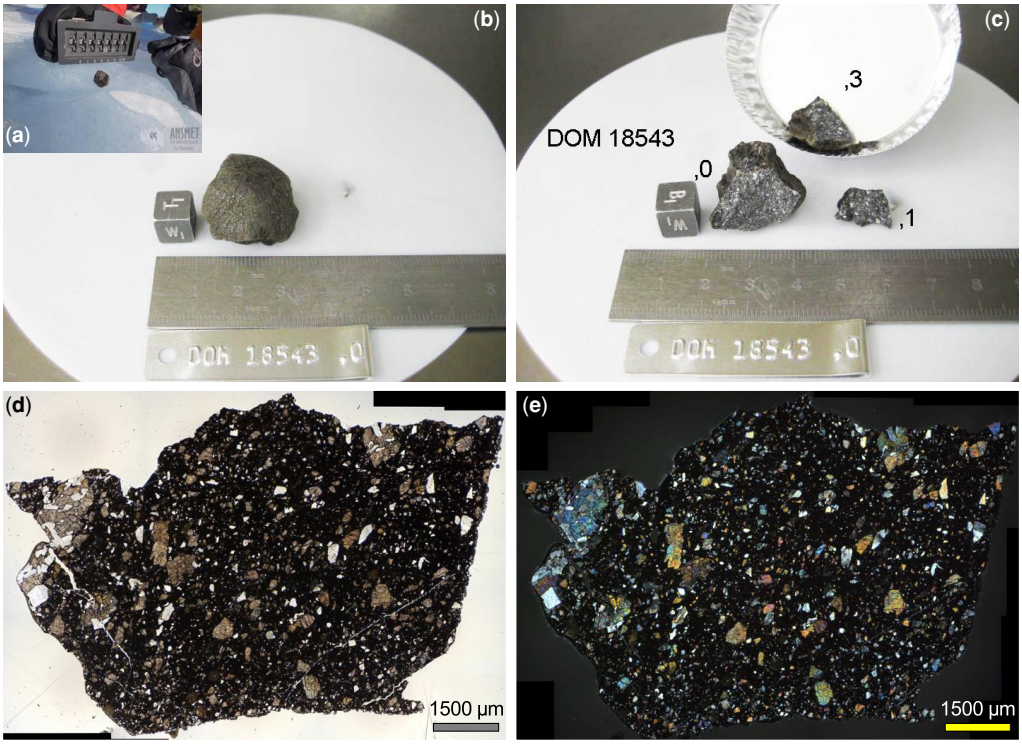


**Fig. 2.** (**a**) Field image of DOM 18543 on the Antarctica ice. Field photo is courtesy of the ANSMET Program, Case Western Reserve University and the University of Utah (see also Satterwhite and Righter (2019), Righter (2024), DOM 18543 and the Lunar Sample Compendium, Righter (2024)). (**b**, **c**) Lab photographs for DOM 18543; (b) top west orientation (Satterwhite and Righter 2019; DOM 18543). (**d**, **e**) DOM 18543,9 in plane-polarized and cross-polarized light, respectively; sample is ~1.2 × ~0.8 cm.

## Analytical methods

Images of DOM 18543,9 were acquired in both plane-polarized light (PPL) and cross-polarized light (XPL) using a Leica DM2700P Petrographic Microscope at Miami University (Fig. 2d, e). Sample characterization via PPL and XPL assisted in the identification and classification of clast types, individual mineral fragments, modal proportions and initial documentation of textures. Acquired images were subsequently utilized to identify regions for investigation via scanning electron microscopy energy dispersive spectroscopy (SEM-EDS) and electron micro-probe analysis (EPMA). Back-scatter electron (BSE) images were acquired on a Zeiss Supra 35 variable-pressure field emission gun scanning electron microscope (VP-FEG-SEM) at the Miami University Center for Advanced Microscopy and Imaging (CAMI). Images were acquired using an accelerating voltage of 25 keV with a working distance of 10.0 mm, and a 120 µm aperture. Semi-quantitative elemental data were collected utilizing a Bruker Xflash 5010 energy dispersive X-ray spectroscope (EDS). *In situ* major elemental analysis of select clasts, mineral fragments, melt veins and the fusion crust was conducted via EPMA on a JEOL JXA-8230 electron micro-probe at the Chevron Geomaterials Characterization Lab at Louisiana State University. Instrument analytical parameters included an accelerating voltage of 15 keV, a 20 nA beam current and spot size of 1 µm for olivines and pyroxenes, and 5 µm for plagioclase feldspars, apatites, melt veins and the fusion crust. A 40 nA beam current and spot size of 1 µm were used for sulfides and oxides. A mixture of natural and synthetic standard reference materials were used in the calibration of the EPMA, details of which are given in the supplementary material.

## Results

### Microscopy

DOM 18543,9 is a basaltic polymict regolith breccia with a fusion crust of varying thickness (0.1–

0.3 mm) surrounding ~60% of the thin section edge. It is composed of <10% clasts enclosed within a variably brecciated, glassy, porphyritic matrix containing individual euhedral to anhedral mineral fragments and clast fragments (Figs 2d, e & 3). Three gabbroic clasts (A, B, C, Fig. 3), the largest being 0.3 cm in length (Clast A, Figs 3 & 4a), were identified and are characterized by plagioclase, clinopyroxene, and variable proportions of minor olivine, ilmenite, silica and trace FeS.

The modal mineralogy of these clasts in DOM 18543,9 was determined using the open-source image processing software ImageJ, following a protocol outlined by Schneider *et al.* (2012). Clast A (Fig. 4a) is composed of 53% pyroxene, 46.5% plagioclase and 0.5% ilmenite; Clast B (Fig. 4b) is composed of 53% pyroxene, 23% plagioclase, 15% olivine, 9% silica and <1% FeS; and Clast C (Fig. 4c) is composed of 65% pyroxene, 32% plagioclase and 3% ilmenite. Clast fragments identified within the brecciated matrix include basalts, impact melt rocks (Osinski *et al.* 2025), rare microbreccias and anorthositic granulites, in addition to three-phase symplectites (see Fig. 5). In Figure 5a and b, two basaltic clasts are shown characterized by 72% pyroxene and 28% plagioclase; and 55% pyroxene, 43% plagioclase and 2% ilmenite, respectively. In Figure 5c, a pyroxene-free, ilmenite-rich fragment is shown that consists of 50% olivine, 22% ilmenite, 16% silica, 11% plagioclase and 1% FeS. In Figure 5d, a relatively large olivine (~350 µm in maximum length) is shown associated with silica grains and minor pyroxene. Two examples of impact melt rock clasts (after Osinski *et al.* 2025) are shown in Figure 5e and f, both of which are dominated by euhedral to subhedral plagioclase and minor pyroxene. Figure 5g outlines a microbreccia clast ~850 µm in maximum length. This clast is composed of multiple mineral fragments and several polymineralic clasts within a glassy matrix. Within this microbreccia is a clast fragment ~220 µm in length interpreted to be an anorthositic granulite based on its texture and associated mineralogy (~80% plagioclase). This microbreccia clast is further characterized via SEM-EDS in the accompanying supplementary figure. Figure 5h shows a representative example of one of several three-phase symplectite clasts in DOM 18543,9 composed of pyroxene (42%), olivine (36%) and silica (22%). While clasts of QMD have previously been reported in paired DOM meteorites (Hayden *et al.* 2022*a*, *b*; Hayden 2023), none were observed in DOM 18543,9.

Figure 6 documents the presence of various mineral fragments throughout the brecciated matrix

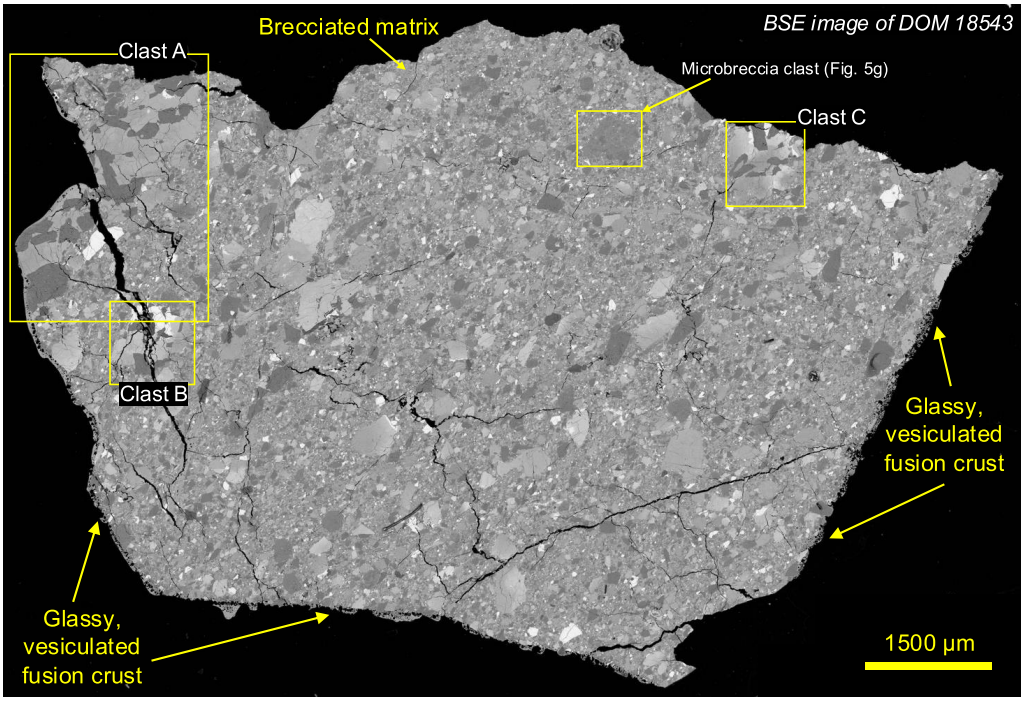


**Fig. 3.** Backscatter electron image of DOM 18543,9. Three gabbroic clasts (A, B, C) are outlined (see Fig. 4) alongside a microbreccia clast (see Fig. 5g).

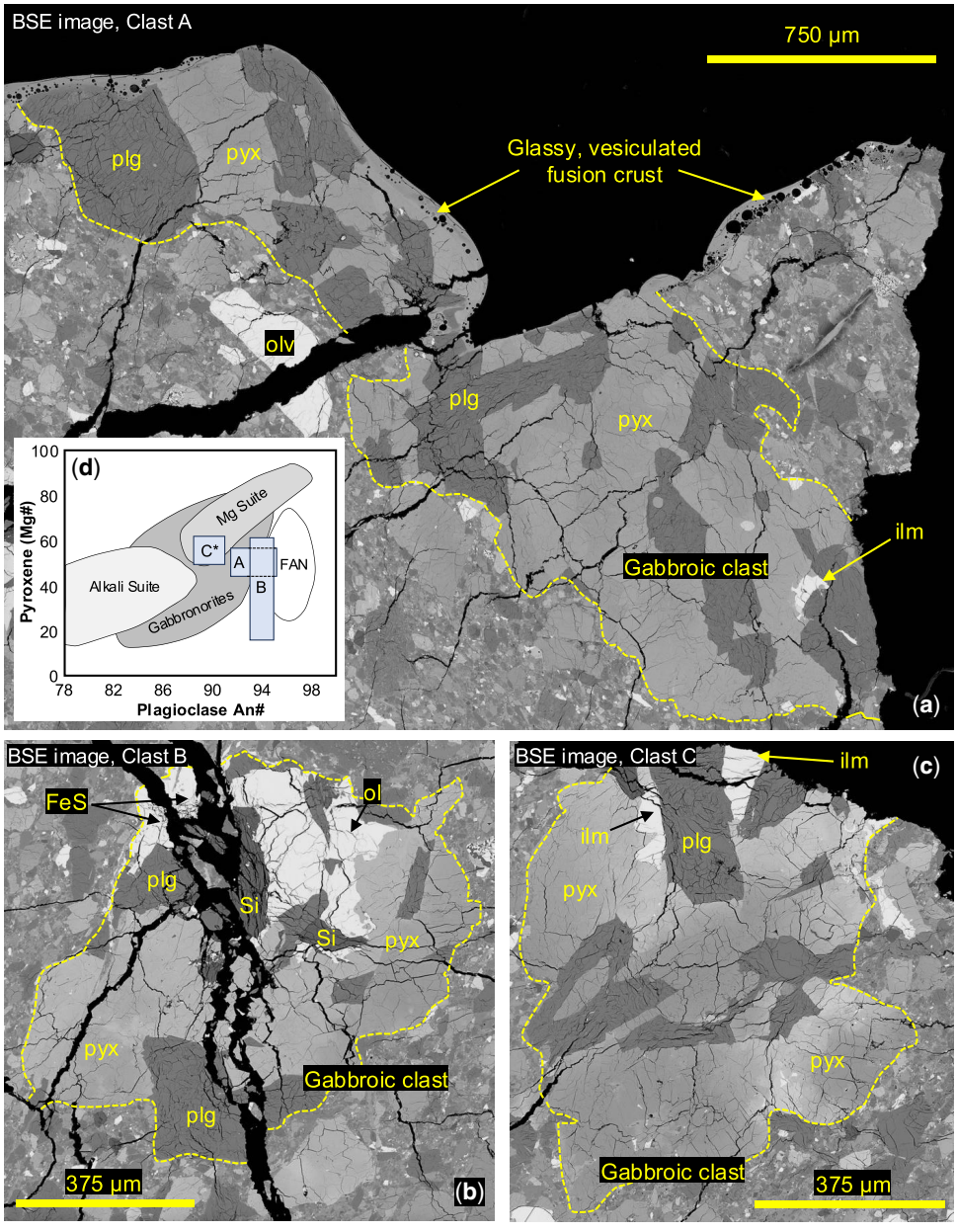


**Fig. 4.** (**a**) Clast A, gabbroic clast: plagioclase and pyroxene with minor ilmenite. (**b**) Clast B, gabbroic clast: pyroxene and plagioclase with minor silica and an FeS-phase and olivine as trace components. (**c**) Clast C, a gabbroic clast: pyroxene and plagioclase with minor ilmenite. (**d**) Plagioclase An# (Ca/[Ca + Na]) v. pyroxene Mg# (Mg/[Mg + Fe]) for lunar lithologies and DOM 18543,9 clasts A–C. C*: two pyroxene analyses yielded Mg# values of 30 and 5. Mineral abbreviations as follows – olv: olivine, plg: plagioclase, pyx: pyroxene, ilm: ilmenite; Si: silica. Source: (c) compositional fields from Lindstrom and Lindstrom (1986) and James *et al.* (1987).

with pyroxene and plagioclase being the most common (subhedral to anhedral; Fig. 6a–c). Silica fragments can be large, up to ~1100 µm in length as shown in Figure 6d although this size is rare. Ilmenite and olivine are present in the matrix as minor components and FeS and apatite grains are

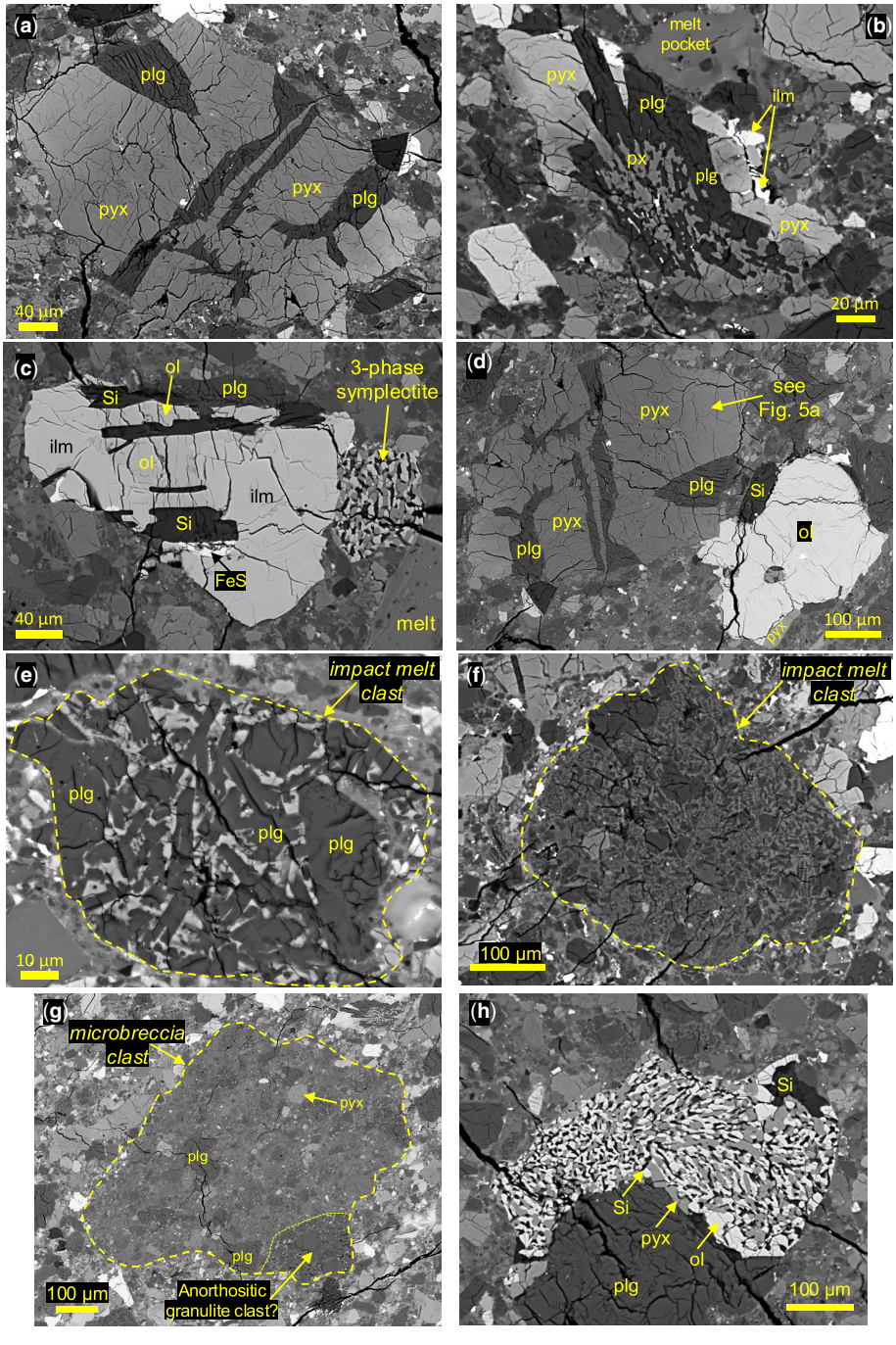


**Fig. 5.** Representative backscatter electron images of the DOM 18543,9 brecciated matrix. (**a**) A pyx–plg basaltic fragment. (**b**) A pyx–plg–ilm basaltic fragment. (**c**) Ilmenite-dominated clast fragment with coexisting olivine (Fe-rich), silica and troilite. A three-phase symplectite clast (fayalite–clinopyroxene–silica) is shown to the right, and a melt pocket in the lower right. (**d**) A pyx–plg basaltic fragment, and olv–Si basaltic fragment. (**e**, **f**) Impact melt clast fragments. (**g**) A plg-rich microbreccia with anorthositic granulite clast. (**h**) Three-phase symplectite (olv–cpx–Si). Mineral abbreviations as follows – olv: olivine, cpx: clinopyroxene; plg: plagioclase, pyx: pyroxene, ilm: ilmenite; Si: silica.

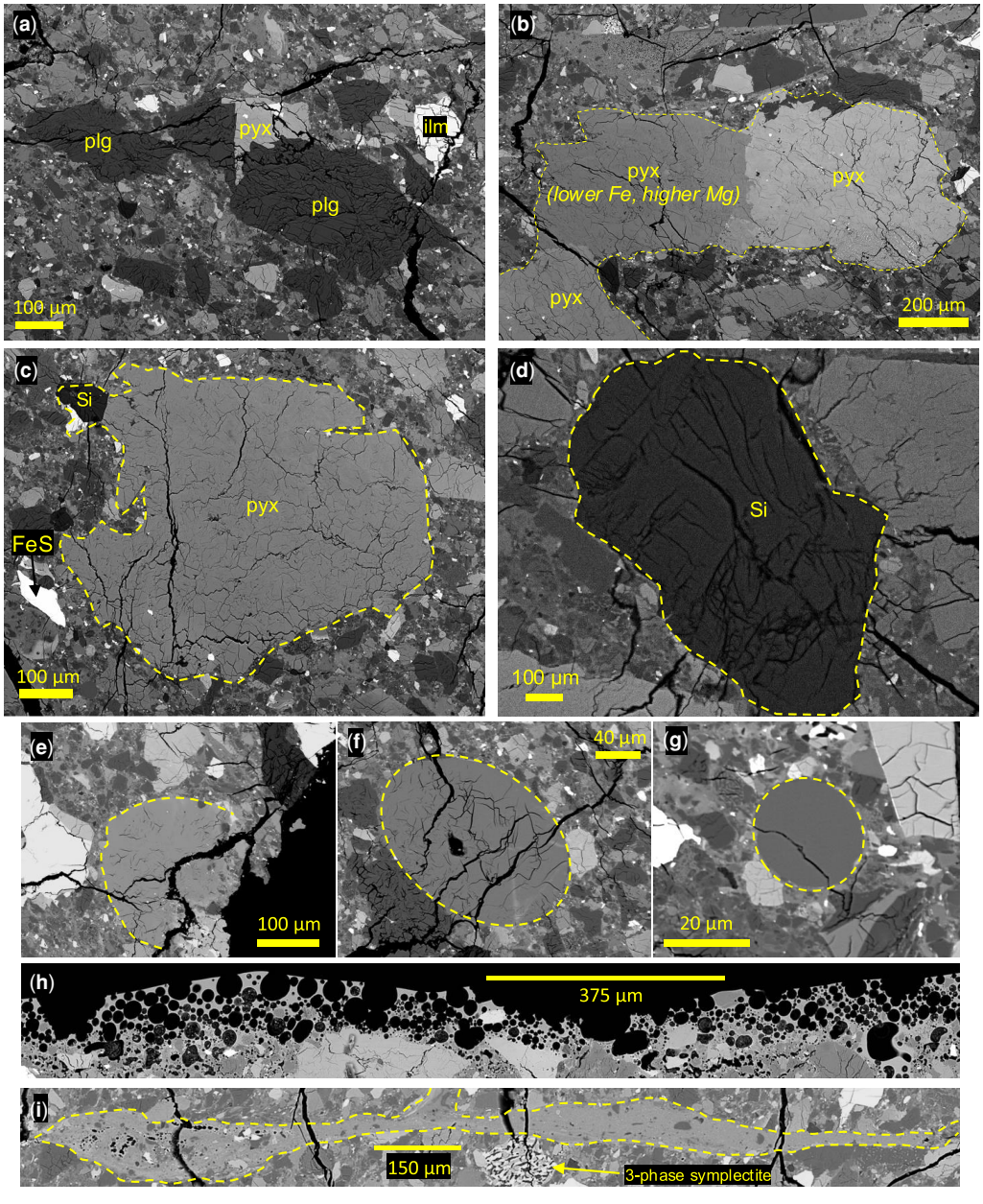


**Fig. 6.** Representative backscatter electron images of the DOM 18543,9 brecciated matrix (continued from Fig. 5). (**a**) Pyroxene, plagioclase and ilmenite mineral fragments. (**b**) Pyroxene mineral fragments. (**c**) Pyroxene, ilmenite and troilite mineral fragments. (**d**) Large silica mineral fragment. (**e**–**g**) Flass (melt) spherules. (**h**) Highly vesiculated glassy fusion crust. (**i**) Melt pocket. Mineral abbreviations as follows – plg: plagioclase, pyx: pyroxene, ilm: ilmenite; Si: silica.

rare. Figure 6e–g document the presence of variably sized impact glass spherules which are found throughout the matrix, range in shape from spherical to ovular and reach up to ~200 µm in length (see also Gugino *et al.* 2024*a*, *b*). The fusion crust (see Fig. 6h) is highly vesiculated and varies in thickness up to ~200 µm. Figure 6i shows an example of one of the many pervasive melt veins within the matrix (see also local melt pocket in Fig. 5b).

## Electron probe microanalysis

Data collected via EPMA are compiled and available within the supplementary material. Figure 7 shows Fe (a.f.u.) v. Mn (a.f.u.) for a range of planetary objects and the compositional field for lunar meteorites (Curran *et al.* 2019). The Fe–Mn systematics reflect heating during the early Solar System where inner bodies are relatively depleted in volatile components (i.e. Mn), resulting in lower Mn/Fe values when compared to more distant objects (e.g. Mars, Vesta; Taylor 1992; Wang and Jacobsen 2016; Steenstra *et al.* 2018). As shown, the Moon is characteristically Mn-depleted, which is attributed to further volatile loss during the Moon-forming giant impact event (e.g. Papike *et al.* 2003; Karner *et al.* 2006; Canup 2012; Canup *et al.* 2015). From Figure 7, DOM 18543,9 pyroxenes from igneous clasts, and pyroxenes that exist as mineral fragments within the brecciated matrix, are consistent with the lunar Mn/Fe trend, and the lunar meteorite field. Figure 8 summarizes the En–Fs–Wo systematics for DOM 18543,9 pyroxenes where the majority are augite or pigeonite compositions with rarer En-rich grains ($n = 3$, Fig. 8b). In Figure 8c–e, the inter- and intra-grain variability is illustrated with the pyroxene in Clast C (Fig. 8e) ranging from $En_4Fs_{69}Wo_{27}$ to $En_{47}Fs_{29}Wo_{24}$, which encompasses close to the entire range of compositions exhibited by all DOM 18543,9 pyroxenes.

Figure 9 summarizes the An–Ab–Or systematics for DOM 18543,9 plagioclase grains, which are predominantly anorthitic ($\geq An_{90}$). Of particular note is the composition of plagioclase grains with $>An_{95}$ which, within a lunar framework, are typically consistent with FAN-related lithologies. These An-rich compositions are found throughout the sampled plagioclase populations (Fig. 9a–c), including mineral fragments within the brecciated matrix. In Figure 9d, several anorthite grains within the microbreccia clast are shown, two of which are associated with a clast fragment interpreted to be an anorthositic granulite (see Fig. 5g, see also: Supplementary Figure). In Figure 9e the compositions of anorthites from this microbreccia are shown on the lunar plagioclase An# v. pyroxene Mg# framework, where their average An content ($An_{96.3}$) is generally consistent with FAN compositions within the lunar highland frameworks of Lindstrom and Lindstrom (1986) and James *et al.* (1987) (see Discussion section). Also shown are anorthite data for gabbroic clasts A, B and C, all of which plot to the left of the FAN field and are more compositionally consistent with lunar gabbronoritic compositions (see Fig. 4d). While it is noted here that Ca-rich plagioclase ($>An_{95}$) has been documented to occur within some Apollo basalts (Papike *et al.* 1991), the Mg# values of the plagioclase grains within clasts A, B and C range from 12 to 27, with one exception at Mg# 73 (see supplementary material and Discussion below).

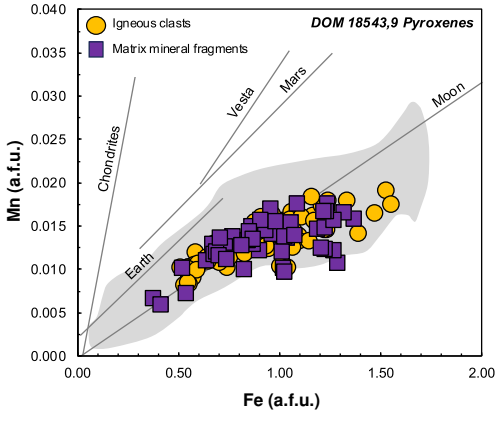


**Fig. 7.** Fe (atoms per formula unit; a.f.u.) v. Mn (a.f.u.) for DOM 18543,9 pyroxenes. Compositions are consistent with the lunar trend. Source: Fe/Mn planetary fractionation from Papike *et al.* (2003), based on four oxygens; grey-filled field represents lunar meteorite data from the literature as summarized in Curran *et al.* (2019).

Figure 10 summarizes the compositions of DOM 18543,9 olivines, which are predominantly Fe-rich ($\geq Fa_{85}$). The only exceptions to this are two analyses of one olivine mineral fragment that yielded $Fo_{51}$-$Fa_{49}$ compositions (see Fig. 10b). Olivine in Clast B yielded $Fo_5Fa_{95}$ ($n = 3$); all other olivine analyses are associated with mineral fragments within the brecciated matrix and are also fayalitic. The compositions of spinels are shown in Figure 11 on a 2*Ti–Cr–Al ternary diagram and summarized by FeO/(FeO + MgO) v. $TiO_2/(TiO_2 + Al_2O_3 + Cr_2O_3)$ systematics. In both cases, compositions are shown in comparison to Apollo 12 and Apollo 15 spinels (after Anand *et al.* 2006). While DOM 18543,9 spinel analyses are limited, the majority are ulvöspinels ($n = 6$) with rarer chromite ($n = 1$). Figure 12a shows the compositions of DOM 18543,9 apatite plotted in OH–F–Cl ternary space ($n = 7$). All grains are fluorapatites with compositions consistent with crystallization from a basaltic melt where $H_2O >$ Cl > F (McCubbin *et al.* 2011). Figure 13a summarizes the chemical composition of the glassy fusion crust and melt pockets throughout the brecciated matrix of DOM 18543,9. As shown in Figure 13a, glasses are basaltic with low total alkalis: <52 wt% $SiO_2$ and <0.3 wt% $Na_2O + K_2O$. In Figure 13b and c, select locations at which the fusion crust in DOM 18543,9 was analysed are shown. In Figure 13b fusion crust glasses are relatively FeO-rich (up to 37.4 wt%) due to the decomposition of ilmenite compared to those in Figure 13c where FeO contents are more similar to those of the melt pockets throughout the matrix (Fig. 13a).

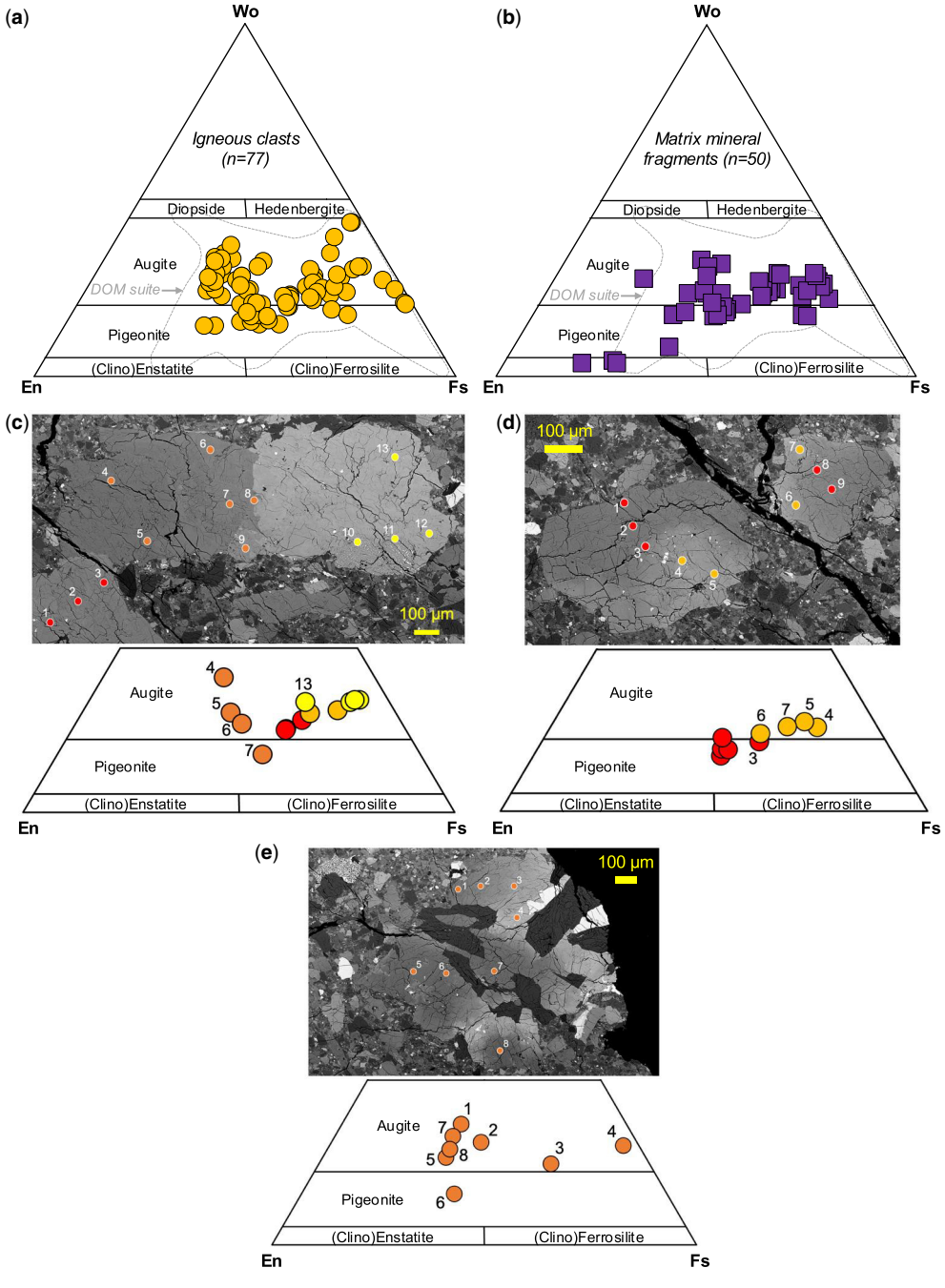


**Fig. 8.** Clinopyroxene En–Fs–Wo ternary diagrams. (**a**) DOM 18543,9 igneous clast clinopyroxenes with the compositional field clinopyroxenes from paired DOM suite basaltic meteorites also shown: DOM 18509, 18543 and 18678 (Gross *et al.* 2020), and DOM 18262 and 18666 (Hayden *et al.* 2022*a*). (**b**) DOM 18543,9 clinopyroxene mineral fragments from the brecciated matrix. Compositional field data for DOM as in (a). (**c**)–(**e**) Clinopyroxene compositions in clasts A–C (see Figs 3 & 4). The numbered locations and colours on the backscatter electron (BSE) images correspond to the numbers and colours on the associated clinopyroxene ternary diagram below each BSE image. Different colours were used in (c) and (d) to better visualize the compositional variation that exists within the grain.

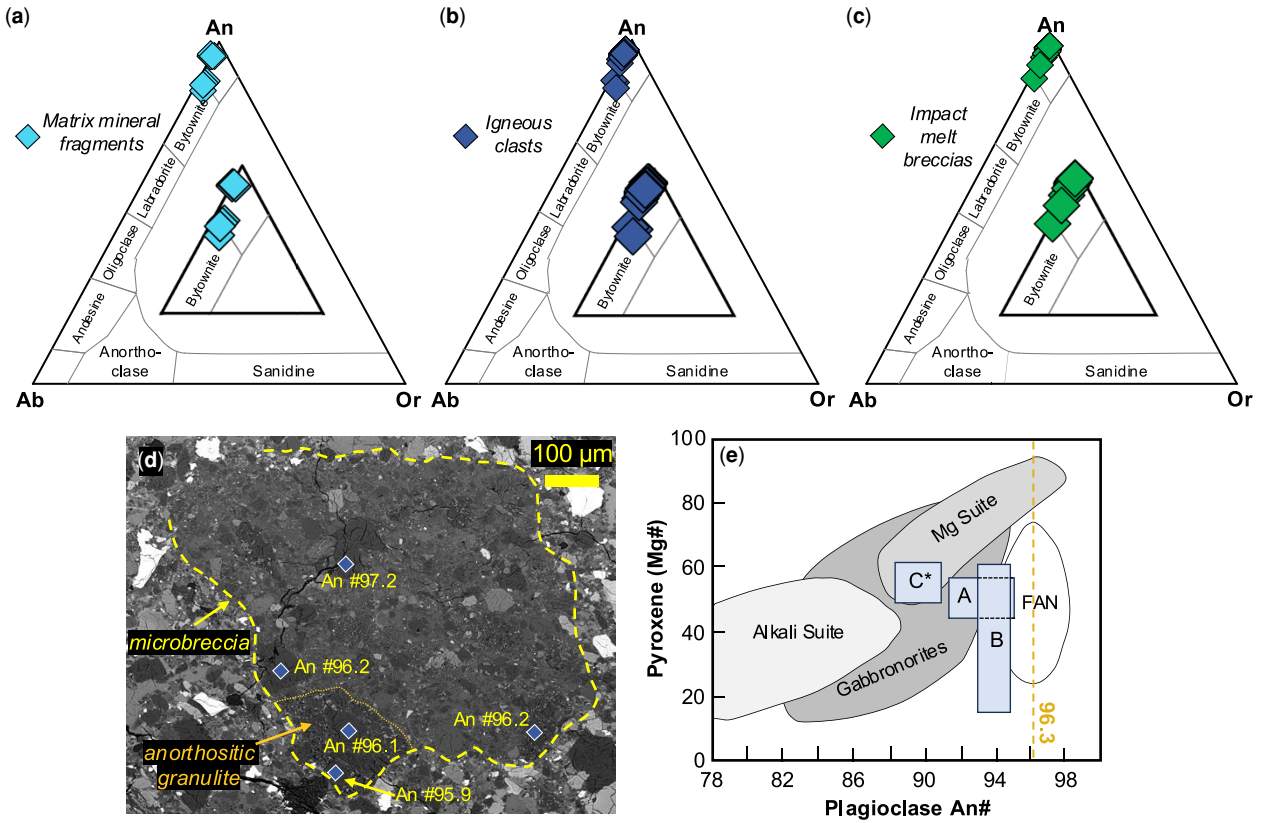


**Fig. 9.** (**a**)–(**c**) Plagioclase An–Ab–Or ternary diagrams for DOM 18543,9 plagioclase feldspars with insets from $An_{80}$ to $An_{100}$. (a) Mineral fragments within the brecciated matrix. (b) Igneous clast plagioclase, including within the microbreccia clast fragment (see panel **(d)** and Figure 5f). (c) Impact melt clast plagioclase. (**d**) Plagioclase An contents within the microbreccia clast, with a probable anorthositic granulite clast outlined. (**e**) Plagioclase An# (Ca/[Ca + Na]) v. pyroxene Mg# (Mg/[Mg + Fe]) for lunar lithologies. The composition of plagioclase in the gabbroic clasts (A, B, C; Fig. 3) are shown alongside the average of plagioclase An content ($An_{96.3}$) from the microbreccia in (d). Source: (e) compositional fields from Lindstrom and Lindstrom (1986) and James *et al.* (1987).

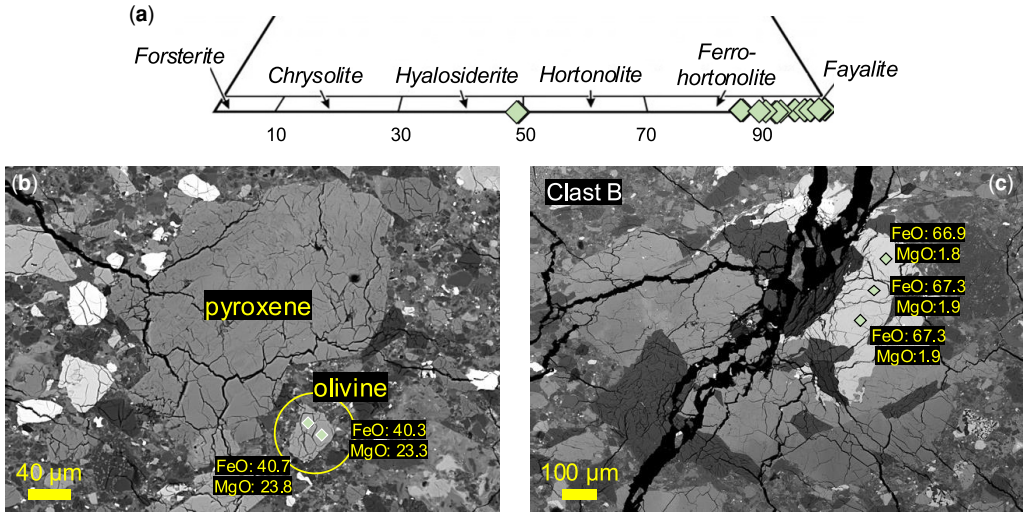


**Fig. 10.** (**a**) Compositions of DOM 18543,9 olivine plotted on the olivine ternary diagram ($n = 24$). (**b**) Matrix olivine ($Fo_{51}Fa_{49}$, $n = 3$). (**c**) Fe-rich olivine in Clast B, $Fo_5Fa_{95}$ (see also Figs 3 & 4b).

In summary, DOM 18543,9 is composed of basaltic materials, predominantly clinopyroxenes of augite and pigeonite composition, anorthitic plagioclase, Fe-rich olivines and rare orthopyroxenes. The silicate mineralogy and geochemistry is therefore consistent with initial work on this DOM meteorite suite (Gross *et al.* 2020; Zeigler *et al.* 2021). The presence of rare anorthositic granulite clasts with FAN-like plagioclase compositions does, however, support the presence of non-mare materials at the meteorites' source region on the lunar surface.

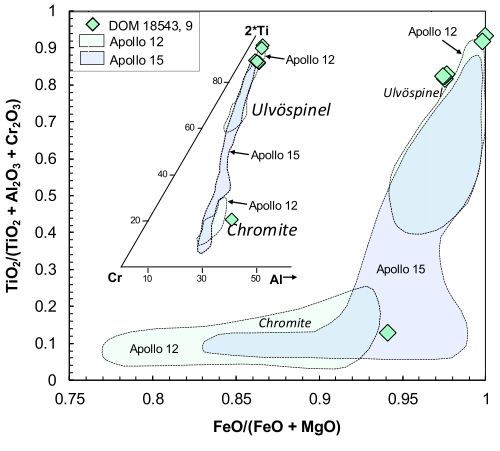


**Fig. 11.** FeO/(FeO + MgO) v. $TiO_2/(TiO_2 + Al_2O_3 + Cr_2O_3)$ systematics for DOM 18543,9 spinels ($n = 7$) shown with the 2*Ti–Cr–Al (in mol.%) ternary diagram. Source: modified from Anand *et al.* (2006) with Apollo 12 and 15 spinel data from El Goresy (1976).

# Discussion

## Comparison of DOM 18543,9 to Apollo and Chang'e basalts

The predominance of basaltic materials in DOM 18543,9 implies derivation from a mare-dominated terrane on the lunar surface. The spatial and temporal distribution of basaltic magmatism on the Moon has

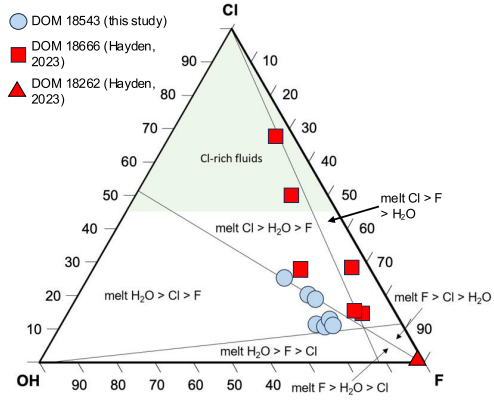


**Fig. 12.** OH–F–Cl ternary for apatite with OH calculated based on apatite stoichiometry (Ketchum 2015). Data from DOM 18543 are shown by light blue circles with all compositions consistent with fluorapatite. Also shown are apatite data from paired 2018–19 DOM lunar meteorites with DOM 18666 ranging from chlorapatite to compositions similar to those in DOM 18543. One analysis from DOM 18262 is also shown (Cl-poor). Source: compositional fields after McCubbin *et al.* (2011).

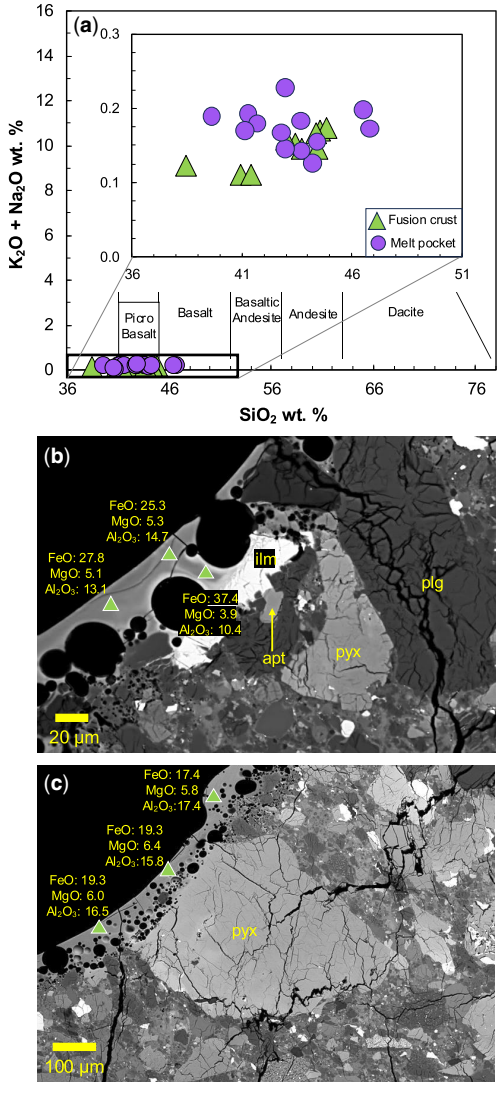


**Fig. 13.** (**a**) $SiO_2$ v. $Na_2O + K_2O$ (wt%) for DOM 18543,9 fusion crust ($n = 9$) and melt pockets throughout the brecciated matrix ($n = 13$). Glass compositions are basaltic and low alkali (all $Na_2O + K_2O$ <0.3 wt%). (**b**, **c**) Backscatter electron images of the fusion crust and location of several electron microprobe analyses with select major oxides reported in wt%. Mineral abbreviations as follows – olv: olivine, plg: plagioclase, pyx: pyroxene, ilm: ilmenite; Si: silica, apt: apatite.

historically been interpreted to result from heat-producing elements that would have supported (1) peak lunar volcanism from ~3.8 to 3.3 Ga and subsequent decline in eruptive activity, and (2) associated models of mantle thermal evolution (Shearer *et al.* 2006; Ziethe *et al.* 2009; Laneuville *et al.* 2018). Within this framework, the Apollo high-Ti basalts are broadly constrained to ~3.6–3.8 Ga while the low-Ti basalts are broadly constrained to ~3.1–3.3 Ga (Snape *et al.* 2019). More recently, however, a relatively protracted record of basaltic volcanism to ~2 Ga has been confirmed by analysis of the Chang'e 5 basalts, which yielded Pb–Pb ages of 2.03 ± 0.004 Ga (Che *et al.* 2021; Li *et al.* 2021; Tian *et al.* 2023) and 1.96 ± 0.09 Ga (Shen *et al.* 2024). From the Chang'e 6 mission, basalts from the lunar farside yielded two distinct ages: 4.2 Ga for a high-Al basalt and 2.8 Ga for a low-Ti basalt (Cui *et al.* 2024; Zhang *et al.* 2024; Che *et al.* 2025; Shen *et al.* 2025), which now represents the oldest example of basaltic magmatism on the Moon (Zhang *et al.* 2024).

The compositions of pyroxene, ilmenite and olivine in DOM 18543,9 are now considered within the geochemical framework of the Apollo and Chang'e basalts. Through this comparative approach, the origin of DOM 18543,9 materials is considered and placed within the context of lunar basaltic volcanism.

In Figure 14a, the En–Fs–Wo systematics of pyroxenes from basalts associated with Apollo 11, 12, 14, 15, 16 and 17 missions are summarized (open and filled symbols, data compilation from https://www.astromat.org and numerous references therein). Pyroxenes from the Chang'e 5 and 6 missions are shown as compositional fields (Shen *et al.* 2025; Yin *et al.* 2025). The majority of lunar pyroxenes are augites and pigeonites with significant En–Fs–Wo compositional overlap between missions. In Figure 14b, the systematics of lunar clinopyroxene Fe# v. Ti# is summarized where Fe# = mol. ratio of $Fe/(Fe + Mg)$ and Ti# = mol. ratio of $Ti/(Ti + Cr)$. Clinopyroxenes associated with high-Ti, low-Ti and very low-Ti basalts are shown as compositional fields after Arai *et al.* (2010) with the more recent Chang'e 5 and 6 data also shown as discrete fields after Tian *et al.* (2023) and Yin *et al.* (2025). For pyroxenes associated with low-Ti and very low-Ti basalts, pyroxene Ti# and Fe# are positively correlated. For high-Ti group pyroxenes, Ti# exhibits little variation with increasing Fe#. The compositional trends produced as pyroxene crystallizes are influenced by the bulk composition of their source magma(s) with Fe# increasing along with Ti# as pyroxene crystallization proceeds, until an Fe–Ti mineral crystallizes (Robinson *et al.* 2012). In this scenario, early-formed pyroxenes have the lowest Fe# contents. For high-Ti basalts, Fe–Ti minerals (e.g. ilmenite) are the liquidus, or near-liquidus, phases and thus lead to co-crystallized pyroxenes with near-constant Ti# values (e.g. Grove and Beaty 1980; Robinson *et al.* 2012).

The DOM 18543,9 pyroxenes are consistent with derivation from a low-Ti basaltic source. Pyroxenes from Apollo samples that are typical of the very

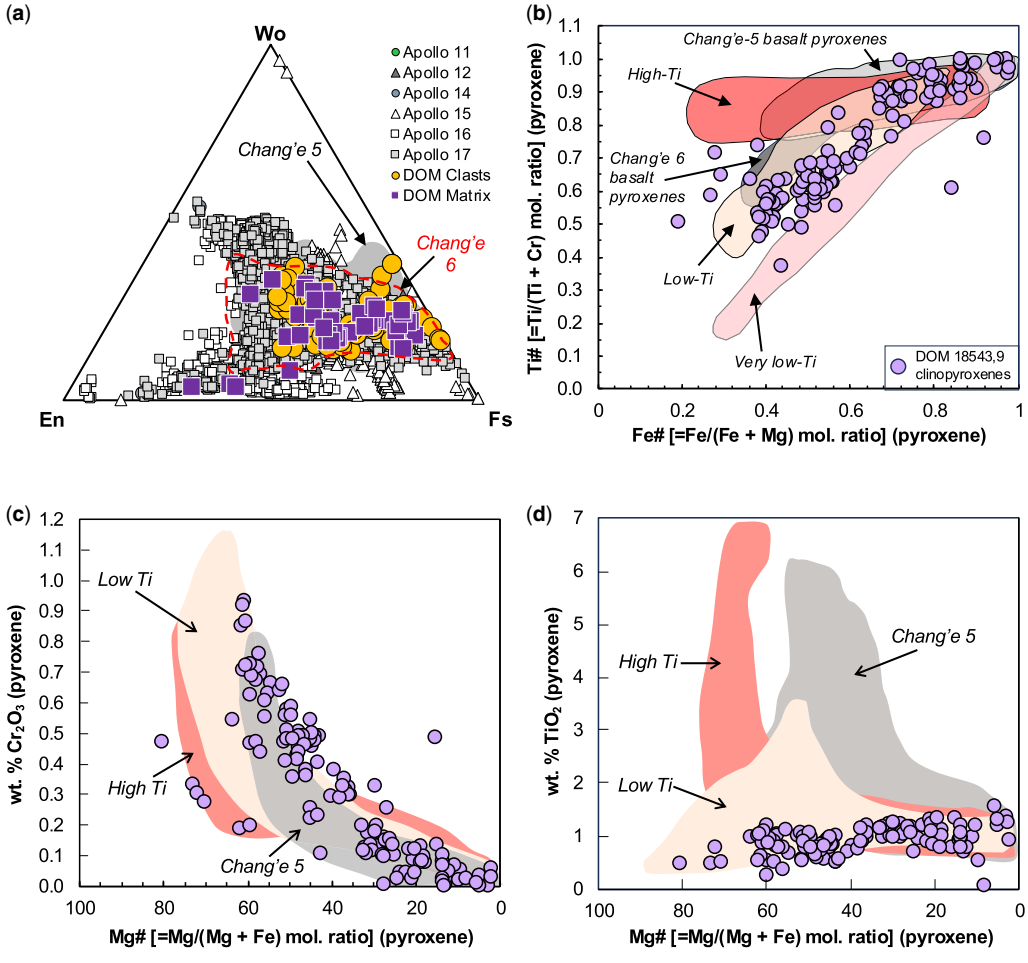


**Fig. 14.** (**a**) En–Fs–Wo compositions of DOM 18543,9 pyroxenes from igneous clasts and mineral fragments shown in comparison to Apollo pyroxenes. Note, pyroxene data from Chang'e 6 soils are presented in C. Li *et al.* (2024) and extend to more En-rich, Ca-poor compositions. (**b**) Fe# v. Ti# for DOM 18543,9 pyroxenes compared to high-Ti, low-Ti and very low-Ti compositions fields for Apollo basalt pyroxenes. (**c**) Mg# v. wt% $Cr_2O_3$. (**d**) Mg# v. wt% $TiO_2$ in DOM 18543,9 pyroxenes compared to low-Ti and high-Ti Apollo compositional fields, and Chang'e 5 pyroxenes. Source: Apollo data from AstroMat; Chang'e 5 and Chang'e 6 compositional fields from Yin *et al.* (2025), and see also Shen *et al.* (2025); (b) after Arai *et al.* (2010), Chang'e 5 pyroxene field after Tian *et al.* (2023), and Chang'e 6 pyroxene field after Yin *et al.* (2025); (c) compositional fields from Tian *et al.* (2023).

low-Ti basalt field are predominantly associated with basaltic material Apollo 16 samples (Taylor *et al.* 1977; Haskin and Warren 1991) while Apollo pyroxenes with a low-Ti composition are typically associated with Apollo 11, 12 and ±15 samples (Haskin and Warren 1991). Pyroxenes associated with the high-Ti basalt field are largely constrained to Apollo 14 and 17 samples (Shih *et al.* 1975; Giguere *et al.* 2000). The geochemical similarity between DOM 18543,9 clinopyroxenes and those of low-Ti basalts is further exemplified in Figure 14c and d, which consider Mg# v. wt% $Cr_2O_3$ systematics, and Mg# v. wt% $TiO_2$ systematics. While wt% $Cr_2O_3$ signatures are similar across lunar clinopyroxene groups, the Mg# values of DOM 18543,9 clinopyroxenes are more similar to those of the low-Ti basalts (Fig. 14c), with wt% $TiO_2$ signatures clearly distinguishable from those of the high-Ti and Chang'e 5 compositional fields. Where wt% $Cr_2O_3$ contents in pyroxene decrease with decreasing Mg# (Fig. 14c), co-crystallization of Cr-rich spinel is inferred (Tian *et al.* 2023).

In Figure 15a, multiple spot analyses of one ilmenite grain from DOM 18543,9 are shown. In

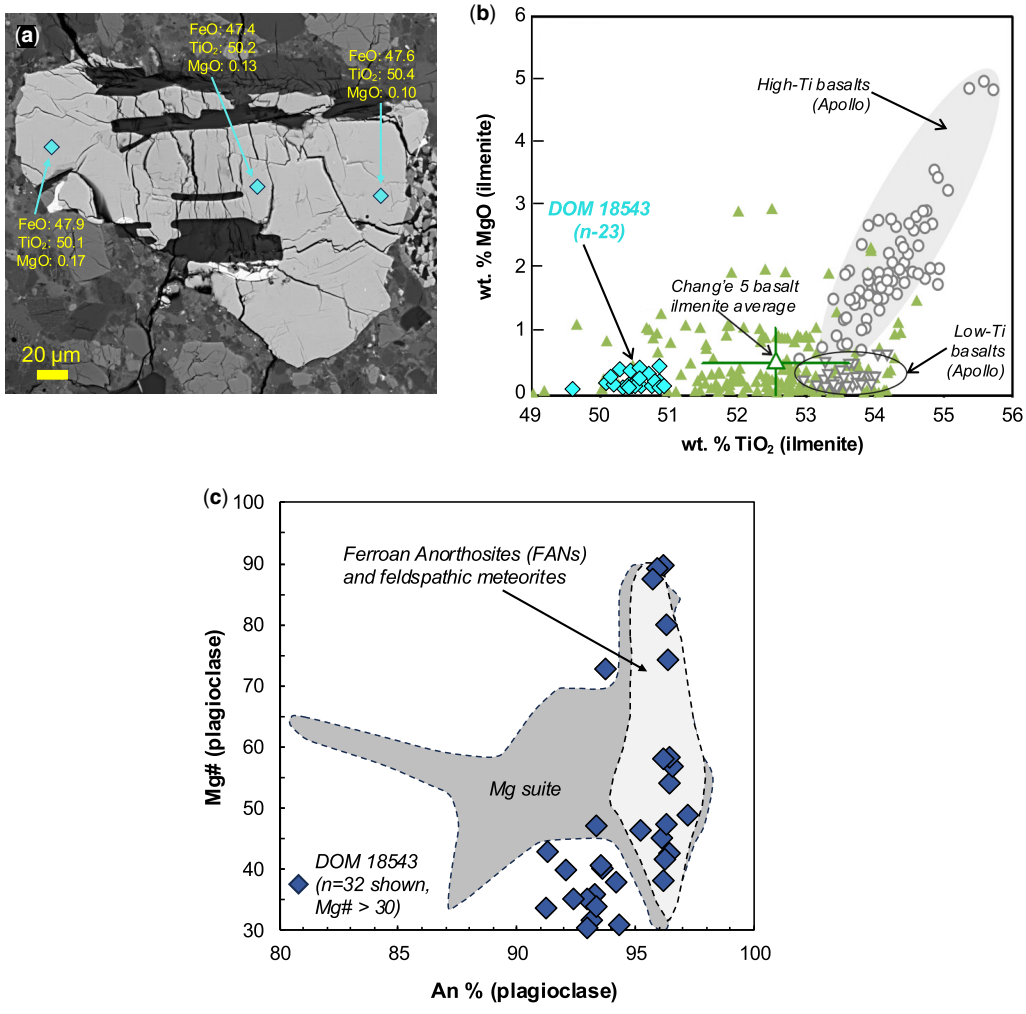


**Fig. 15.** (**a**) Location of three spot analyses of one (relatively large) ilmenite grain; see also Figure 5c. (**b**) $TiO_2$ v. MgO (wt%) for lunar ilmenites. DOM 18543,9 ilmenites in both clasts and mineral fragments exhibit comparatively low wt% $TiO_2$ compared to low-Ti Apollo basalts, high-Ti Apollo basalts and Chang'e 5 basalts. (**c**) An (%) v. Mg# for DOM 18543,9 plagioclases, for Mg# >30 ($n = 32$ of 51 analyses). Note the Mg# of plagioclases in clasts A, B and C range from 12 to 27 and are not shown (see text for discussion). As shown, many of the plotted feldspars exhibit Mg# >30 at An > 95%, consistent with derivation from feldspathic materials. Source: (b) modified from Tian *et al.* (2023); (c) modified from Pernet-Fisher *et al.* (2017)

Figure 15b, all DOM 18543,9 ilmenite analyses are shown in comparison to ilmenite from the Apollo high-Ti and low-Ti basalts, in addition to the Chang'e 5 basalts (Tian *et al.* 2023). The low $TiO_2$ contents (≤51 wt%) combined with the low MgO values (<1 wt%) of DOM 18543,9 ilmenites are consistent with relatively late-stage ilmenite crystallization, and relatively late-stage magmatic differentiation. From Figure 5a and c, relatively late-stage fractionation is consistent with the co-occurrence of silica and Fe-rich olivine, and consistent with the recent experimental work of Schmidt and Kraettli (2022) where lunar basaltic melts were shown to converge towards similar cotectics in a dry, tholeiitic magmatic environment: pyroxene–plagioclase–quartz (±FeTi-oxide, ±Fe-rich olivine).

In Figure 15c, the An content (%) in DOM 18543,9 plagioclase is shown alongside corresponding Mg# values. As shown, several of the analysed grains ($n = 16$) are geochemically consistent with derivation from feldspathic materials and overlap the compositional field for FANs and feldspathic

meteorites (Pernet-Fisher *et al.* 2017). The Mg# of the anorthositic granulite and the microbreccia clast (Fig. 9d) are variable: 21–89 and 27–90 respectively. The Mg# (and An%) of plagioclase within the gabbroic clasts (A, B, C) are inconsistent with derivation from FAN-like materials with Mg# often <30. These characteristics support an inference of materials within DOM 18543,9 being sourced from lunar terranes that contain both feldspathic and basaltic, evolved mare materials.

In Figure 16a, a summary of the wt% MgO compositions in Apollo olivines is shown (data compilation from https://www.astromat.org). The inset graph indicates that low wt% MgO, Fe-rich olivines are relatively more common in the Apollo 12 and 15 ($\pm$17) basalts ($n = 48$). In Figure 16b, the wt% MgO compositions of DOM 18543,9 olivines are shown, with the majority exhibiting fayalitic signatures at $\leq$5 wt% MgO ($n = 19$). In Figure 16c and d, the %Fa and %Fo contents of DOM 18543,9 olivines are shown in comparison to a variety of Apollo basalt types (Donohue and Neal 2018). As shown, Fa-rich compositions such as those found in DOM 18543,9 are relatively rare within the Apollo suite. When present in the Apollo basaltic suite, Fa-rich olivine compositions are often associated with mesostasis regions where textures consistent with silicate liquid immiscibility and/or symplectites are also found (e.g. Taylor *et al.* 2004; Potts *et al.* 2016). Similarly, recent work on the Chang'e 5 basalts has reported the presence of fayalitic olivines ($Fa_{95–99}$) in association with mesostasis regions

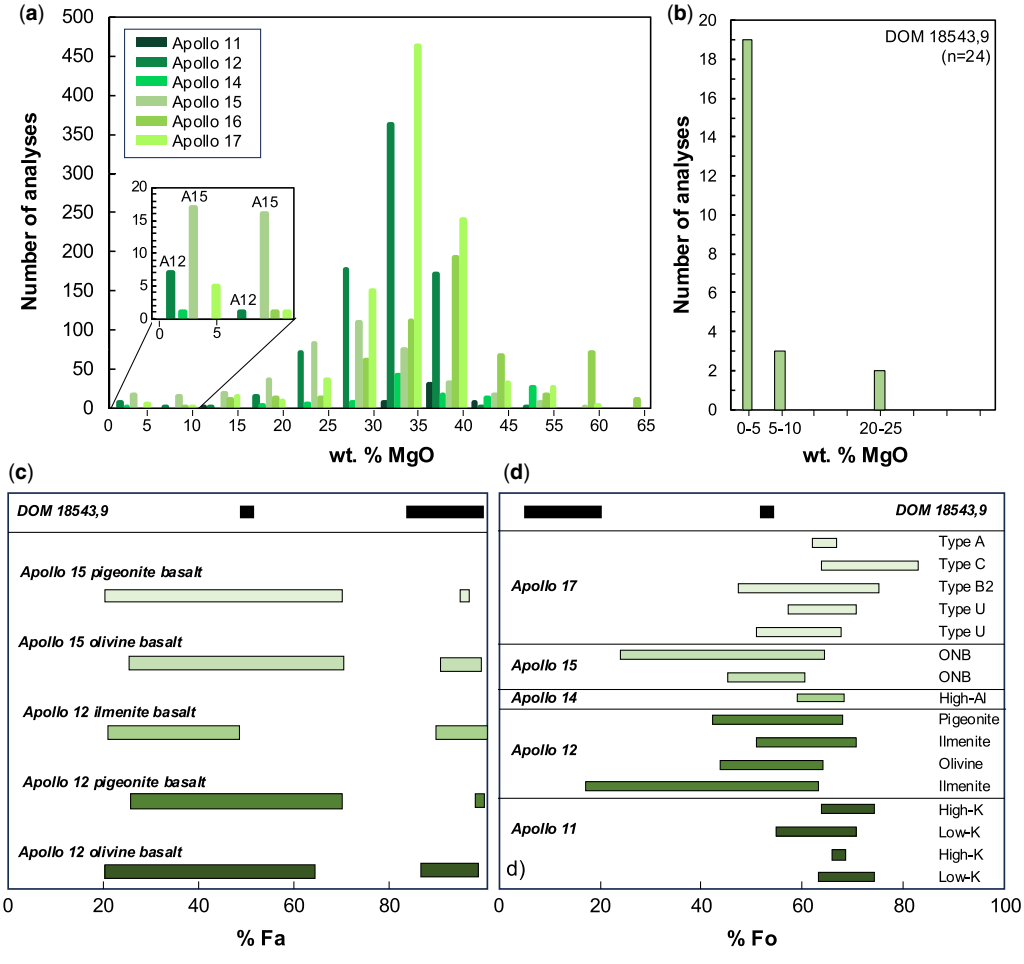


**Fig. 16.** (**a**) Summary of wt% MgO contents of Apollo olivines. Inset graph shows low-MgO olivines ($\leq$10 wt%). (**b**) MgO (wt%) of DOM 18543,9 olivines for comparison. (**c**) DOM 18543,9 olivines compared to Apollo 12 and 15 samples. (**d**) DOM 18543,9 olivines compared to the range of olivine Fo contents from a variety of Apollo samples. Source: data from AstroDB; (c) modified from Haloda *et al.* (2009); (d) after Donohue and Neal (2018).

and attributed their occurrence to late-stage silicate liquid immiscibility (Jin *et al.* 2025; Shen *et al.* 2025; Zhang *et al.* 2024). While Shen *et al.* (2025) reported an absence of olivine in the studied Chang'e 6 basaltic fragments, Zhang *et al.* (2024) reported the presence of Fe-rich olivine in Chang'e 6 poikilitic and subophitic clasts and their association with Zr-rich minerals, apatite, mesostasis and troilite. Subsequently, Sheng *et al.* (2025) reported the presence of primitive, forsteritic olivines in Chang'e 6 soils with inferred Mg-suite and lunar mantle origins. While Fe-rich olivine does occur within three-phase symplectite clasts of DOM 18543,9 (see Fig. 5h), the analyses reported in Figures 15b and 16b are not associated with the symplectites and are all associated with individual mineral fragments and other lithic clast types (Figs 10b, c & 15a). The presence of three-phase symplectite clasts composed of Fe-rich olivine, clinopyroxene and silica in DOM 18543,9 is, however, consistent with their derivation from a relatively evolved basaltic source where magmatic differentiation has led to Fe-enrichment and fayalite, clinopyroxene and silica forming as a late-stage eutectoid composition (Shaulis *et al.* 2017).

Within the context of the Apollo and Chang'e basaltic framework, and from the evaluation of geochemical signatures of pyroxene, ilmenite, plagioclase and olivine, it is therefore likely that the basaltic fragments of the DOM 18543,9 breccia originally crystallized from a compositionally evolved, low-Ti parental magma, and collectively represent the relatively late stages of crystallization.

## Comparison of DOM 18543,9 to the 2018–19 lunar DOM suite

The 2018–19 clan of basaltic lunar meteorites, to which DOM 18543 belongs, have been classified as polymict regolith breccias. The textures, mineralogies and geochemical signatures of DOM 18543,9 reported here support this classification. Clasts in DOM 18543,9 are rare and include basalts, gabbros, impact melt breccias, symplectites and a rare microbreccia that is interpreted to contain FAN-derived material (Fig. 9d, e). From study of paired meteorites DOM 18509, 18543 and 18678, Gross *et al.* (2020) reported clasts of anorthosites, basalts, coarse-grained gabbros, granulites, recrystallized impact melts and symplectites. In addition, the presence of glass spherules accompanied by highly vesiculated fusion crusts and granulite clasts that had been reworked was reported as being consistent with a relatively immature regolith breccia. From characterization of paired meteorites DOM 18509, 18543 and 18678, Zeigler *et al.* (2021) reported basalt clasts, granulitic clasts, anorthosite clasts and silica-dominated clasts with mineral assemblages representative of late-stage mesostasis (alkali feldspar, fayalite, FeTi oxides, high-Ca pyroxene and troilite). From a study of paired meteorite DOM 18262, Hayden *et al.* (2022*a*) reported low- and high-Ti basalt clasts in addition to symplectites and alkali-feldspar-dominated QMDs. In the same study, Hayden *et al.* (2022*a*) also reported basaltic and anorthositic clasts, in addition to microbreccias, in paired meteorite DOM 18666. Characterization of DOM 18666 by McLeod *et al.* (2024) reported $<$10% clasts with basalts, symplectites and impact melt breccias present. All previous work also reports the presence of melt veins of varying thicknesses throughout studied sections in addition to glass spherules. In this study of DOM 18543,9, no granulite and no QMD clasts were identified with anorthositic material constrained to one microbreccia clast (Fig. 9d, e).

In Figure 17a, the compositions of clinopyroxenes from this study and previous studies from which data are available are summarized (Gross *et al.* 2020; Hayden *et al.* 2022*a*). Pyroxenes from DOM 18453 compositionally overlap those from DOM 18262, 18509, 18666 and 18678. From DOM 18262, basalt clast Fe#–Ti# systematics are generally restricted to ~40–50 and ~50–60 while DOM 18666 clast Fe#–Ti# systematics are more variable: ~30–100 and ~50–100, respectively (Hayden *et al.* 2022*a*). Both are consistent with a low-Ti basaltic provenance (see Fig. 14b). From DOM 18509, 18543 and 18678, Zeigler *et al.* (2021) reported plagioclase compositions from $An_{82}$ to $An_{96}$ and olivine compositions from $Fo_1$ to $Fo_{52}$. These anorthite values overlap those in DOM 18543,9 (Fig. 9e) with higher values (~$An_{96}$) similar to those expected in FAN-derived material and consistent with the reported presence of anorthositic highlands material (Zeigler *et al.* 2021). While the olivine compositions also overlap, the majority of DOM 18543,9 olivines are fayalitic (Fig. 10a). Figure 17b summarizes the Cl (ppm) contents of apatite from several of the DOM clan. As shown, these are highly variable with 18543,9 apatites ranging from ~5000 to ~11 000 ppm, 18262 apatites ranging from 0 to ~12 000 ppm (Hayden *et al.* 2022*b*), and apatites from 18666 clustering at ~14 000 ppm (McLeod, unpublished data). This is in contrast to apatite reported for 18666 in Hayden *et al.* (2022*b*), which ranges from ~2000 to ~36 500 ppm Cl. For DOM 18262 and 18666, Hayden *et al.* (2022*b*) also reported $\delta^{37}$Cl and δD for analysed apatites. For $\delta^{37}$Cl, values ranged from −1.0 to +26.0‰ in 18262 and from +5.5 to +19.6‰ in 18666, which are compositionally similar to apatites in high-Ti Apollo 11 basalts, low-Ti Apollo 12 basalts and high-Al Apollo 14 basalts (Hayden *et al.* 2022*a*). For δD, values ranged from −830 to −660‰ for apatite in 18262 ($H_2O$: ~250–

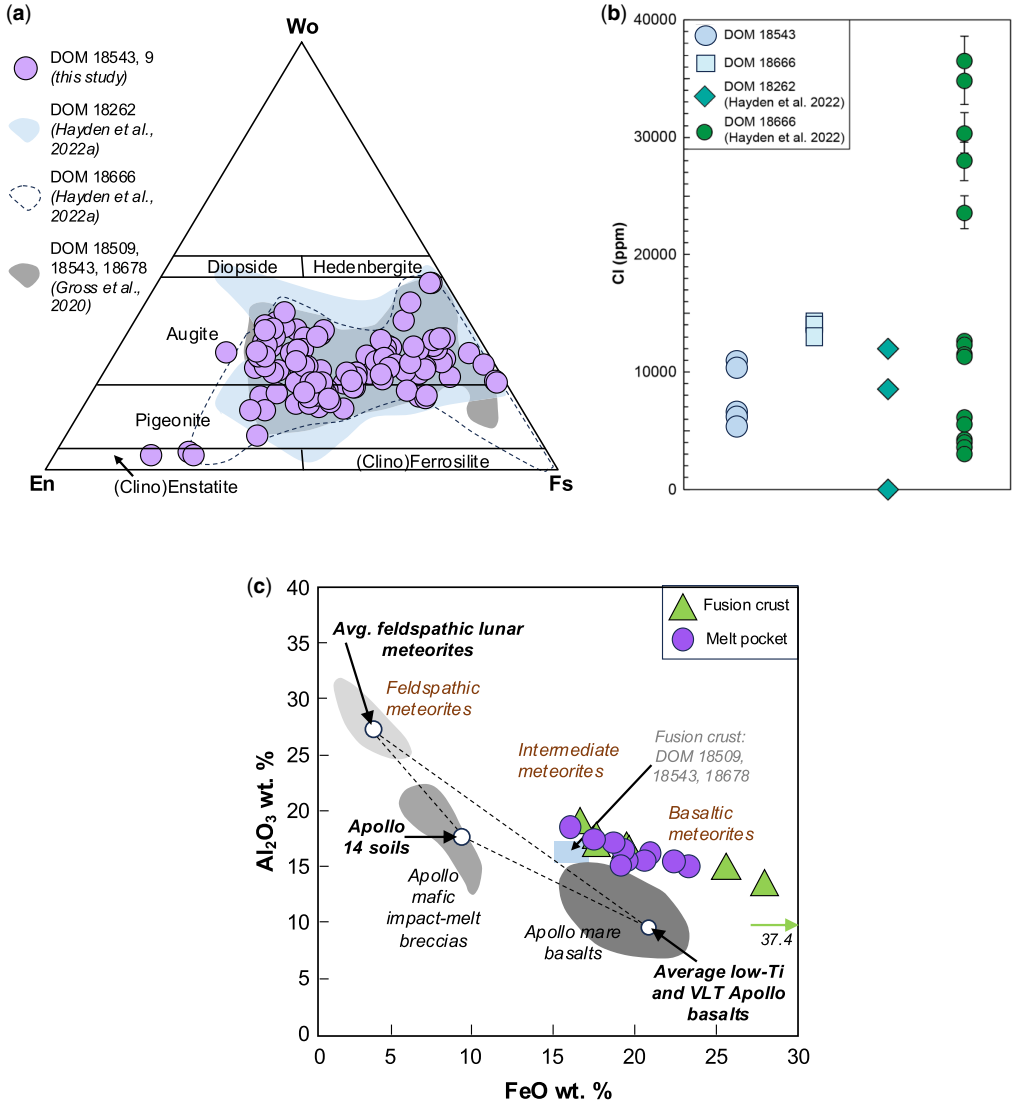


**Fig. 17.** (**a**) Comparison of clinopyroxene compositions shown on an En–Fs–Wo ternary from DOM 18543 (this study), DOM 18509, 18543 and 18678 (Gross *et al.* 2020), and DOM 18262 and 18666 (Hayden *et al.* 2022*a*). (**b**) Comparison of Cl (ppm) contents in apatite from the 2018–19 lunar DOM meteorite suite (Hayden *et al.* 2022*b*, DOM 18666 data from McLeod, unpublished data). (**c**) Glass compositions for DOM 18543,9 plotted in the FeO (wt%) v. $Al_2O_3$ (wt%) framework of Korotev (2005*c*). One analysis of the fusion crust yielded high FeO (37.4 wt%, see panel (c)). Source: (c) modified from Roberts *et al.* (2019); fusion crust data from DOM 18509, 18543 and 18678 from Zeigler *et al.* (2021).

300 ppm) and from −30 to +340‰ for apatite in 18666 ($H_2O$: 1210–3790 ppm). From Hayden *et al.* (2022*b*) and Hayden (2023), the lighter $\delta^{37}Cl$ signatures and the heavier δD signatures in the low-Ti basaltic clasts were compared to those in the Miller Range (MIL) meteorite 05035 due to MIL 05035 being part of the YAMM group of meteorites: Yamato (Y)-793169, Asuka (A)-881757, MET 01210 and MIL 05035. From Hayden *et al.* (2022*b*) and Hayden (2023), the lightest δD signatures were reported to be similar to those in the QMD clasts of the Apollo 15 basalts, and the 2018–19 lunar DOM suite were proposed to be potentially paired with the YAMM group (Robinson

*et al.* 2016; Barrett *et al.* 2023; see discussion below). The anomalously high Cl (ppm) values of apatites in DOM 18666 of Hayden *et al.* (2022*b*) could reflect variations within lunar mantle source regions, in addition to an extreme example of fractional crystallization (Hayden 2023).

For DOM 18543,9 of this study, no QMD clasts were identified. In Figure 17c, the wt% FeO v. wt% $Al_2O_3$ signatures of the DOM 18543,9 fusion crust and melt pockets are used to evaluate lunar provenance (Korotev 2005; Roberts *et al.* 2019). As shown, analysed fusion crust and melt vein glasses are consistent with basaltic meteorite and Apollo mare basalt compositions with slightly elevated wt% $Al_2O_3$ values. Glasses from DOM 18543,9 (alongside 18509 and 18678) also plot towards higher wt% $Al_2O_3$ at lower wt% FeO, consistent with a contribution from feldspathic material and the presence of anorthositic fragments. Specifically, average compositions for the fusion crust in DOM 18509, 18543 and 18678 reported in Gross *et al.* (2020) and Zeigler *et al.* (2021) are as follows: FeO: 15–17 wt%; ferroan: Mg# of 23–24; $Al_2O_3$: 15–17 wt%; $TiO_2$: 1.4–1.8 wt%; and overlap those reported here for 18543,9.

The textural, mineralogical and geochemical similarities between DOM 18543,9 and preliminary study of their pairs to date (18262, 18509, 18666, 18678) support their classification as polymict regolith breccias (e.g. basaltic, gabbroic, symplectitic, impact melt breccia and anorthositic clasts). The compositional similarities of pyroxenes, plagioclase and olivine further support a common, low-Ti basaltic origin, with contributions from anorthositic material. While granulite and QMD clasts are absent from 18543,9, the presence of glass spherules (Fig. 6e–g) and composition of its glass components overlap those of the other DOM meteorites, consistent with a predominantly basaltic provenance, and consistent with the role of regolith processes.

## Evaluating the lunar provenance of the 2018–19 lunar DOM clan

The predominance of basaltic materials in the 2018–19 lunar DOM clan implies derivation from a basaltic terrane, one where regolith and anorthositic materials are locally available. The brecciated nature of the meteorites, in addition to the presence of melt veins, provides insights into the shock conditions under which they formed. All studies to date report the presence of impact glass spherules, melt veins and impact melt breccia clasts, with Hayden *et al.* (2022*a*) specifically reporting fine-grained recrystallization textures alongside melt veins up to 200 μm in width in DOM 18262 and a corresponding shock stage of M-S3/4 (moderately shocked, Stöffler *et al.* 2018; shock stage 2a and 2b after Stöffler and Grieve 2007). This corresponds to equilibration shock pressures between ~20 and 34 GPa and post-shock temperatures up to ~250°C. Hayden *et al.* (2022*a*) also reported moderately shocked conditions (M-S4, shock stage 2b after Stöffler and Grieve 2007) in DOM 18666 on the basis of ~1 mm-wide melt veins and mosaicism in the mafic components. This corresponds to equilibration shock pressures between ~28 and 34 GPa and post-shock temperatures up to ~250°C. In DOM 18543,9, plagioclase grains are often characterized by radial fractures, while glassy, isotropic melt veins throughout the brecciated matrix contain local brecciated zones and regions of mixed melt but are not pervasive (Fig. 6i). Localized mixed melt pockets also exist within the matrix (Fig. 5b, c) but are also not pervasive across the sample. There is no evidence of plagioclase melting to produce vesiculated melt veins, which would otherwise indicate equilibration shock pressures of ~42–45 GPa and post-shock temperatures possibly up to 900°C (stage M-S5; Stöffler *et al.* 2018). It is therefore inferred that DOM 18543,9 experienced similar shock conditions to those of DOM 18262 and DOM 18666 as reported by Hayden *et al.* (2022*a*) and Hayden (2023): moderately shocked and consistent with shock stage M-S4 (Stöffler *et al.* 2018).

The textural features and mineralogical compositions of the DOM clan, in particular 18509, 18543 and 18678, have been compared to those of Meteorite Hills (MET) 01210, which also contains regolith components and granulitic anorthosites. MET 01210 has been interpreted to be derived from a mare region on the lunar surface, and is an immature regolith breccia (Day *et al.* 2006; Joy *et al.* 2010; Zeigler *et al.* 2021). The MET 01210 meteorite is dominated by mare basalt with ~70% of the lithics being basaltic in nature; these are low-Ti to very low-Ti in composition, and are noted as having undergone significant fractionation from their parental magma (Day *et al.* 2006). The remaining ~30% of lithics are composed of granulitic anorthositic clasts, which were noted in Day *et al.* (2006) as being similar in their plagioclase to mafic mineral ratios to granulitic clasts in meteorites MAC 88105 and QUE 93069. Also noted as being present are three-phase symplectite clasts composed of fayalite, clinopyroxene (hedenbergite) and silica, in addition to a range of olivine compositions from $Fo_{94}$ to $Fo_1$ and apatite with 1.7–2.0 wt% Cl. With respect to bulk composition, using the average fusion crust as a proxy, MET 01210 is characterized by 16.2–16.9 wt% FeO and 16.2–17.0 wt% $Al_2O_3$ (Zeigler *et al.* 2005; Day *et al.* 2006), which overlaps that of DOM 18509, 18543 and 18678 (Fig. 17c). Bulk compositions (from powdered chips) for MET 01210 reported by Joy *et al.* (2010) yield 16.5–

17.7 wt% FeO and 14.9–16.6 wt% $Al_2O_3$, which also overlap those of DOM 18509, 18543 and 18678 (Fig. 17c), and with the more feldspathic-rich analyses of DOM 18543,9 glass.

MET 01210 is part of the YAMM group of meteorites, which have been proposed to represent a launch-paired meteorite group from a thick ancient basaltic, low-Ti, KREEP (potassium, rare-earth elements and phosphorus)-poor lava flow in a lunar terrane where anorthositic material is locally available (e.g. Jolliff *et al.* 1993; Koeberl *et al.* 1993; Torigoye-Kita *et al.* 1995; Arai *et al.* 1996, 2010; Huber and Warren 2005; Day *et al.* 2006; Nyquist *et al.* 2007; Zeigler *et al.* 2007; Joy *et al.* 2008, 2010; Fernandes *et al.* 2009; Calzada-Diaz *et al.* 2015; Srivastava *et al.* 2024). More recently, Oliveira *et al.* (2025) recommended that lunar gabbro Ramlat Fasad 532 be added to the YAMM group based on indistinguishable textural, mineralogical and geochemical characteristics. From this, Ramlat Fasad 532 was proposed as being launch-paired with the YAMM group.

Figure 18a compares the olivine compositions in the 2018–19 lunar DOM suite to olivines in several of the YAMM group meteorites, which are highly variable but also include a predominance of fayalitic compositions. Additional comparison of the DOM suite to the YAMM group is shown in Figure 18b, which compares the wt% FeO v. wt% $TiO_2$ bulk rock composition of different Antarctic meteorites to the DOM 18543,9 glass compositions used here as proxies for bulk composition. As shown, the fusion crust and melt pocket compositions of DOM 18543,9 overlap those of the YAMM suite, with one fusion crust analysis overlapping that of the launch-paired YQEN meteorite group (Yamato 793274/981031, EET 87/96, QUE 94281, NWA 4884, ~3.2–3.4 Ga), which is also of mare affinity (Korotev and Zeigler 2014). Also shown at relatively high FeO and $TiO_2$ contents are the NNL launch-paired meteorites (NWA 4734 and NWA 032/479), which are basaltic, are texturally comparable to Apollo 12 and 15 basalts, but are younger (~2.6–3.0 Ga; Korotev and Zeigler 2014). Consistent with observations and geochemical inferences previously discussed for DOM 18543,9, a feldspathic component is present with glass generally exhibiting lower FeO–$TiO_2$ contents within the YAMM field, towards a feldspathic compositional end member (Fig. 18b). In Figure 18c, the magnetic susceptibility (log $\chi$) v. wt% FeO of the 2018–19 DOM clan is shown in comparison to other basaltic and mafic meteorites, in addition to highlands-associated meteorites (Righter *et al.* 2023; Righter 2024). As shown, the DOM clan is distinct from bulk highlands materials, and many other basaltic meteorites. However, it does overlap with MET 01210 and the mare regolith breccia NWA 3136, which is also dominated by basaltic lithics and ~20–30% feldspathic highlands material (Korotev and Irving 2005; Kuehner *et al.* 2005). While a study of separate thin sections of NWA 3136 by Korotev *et al.* (2009) yielded observations 'that are not self-evidently describing the same rock', the bulk wt% $Al_2O_3$ composition of NWA 3136 is comparable to DOM 18543 at ~14% and MET 01210 at 16.2–17.5% (Day *et al.* 2006; Joy and Crawford (2006); O'Donnell *et al.* 2008; Korotev *et al.* 2009). In addition, from Korotev and Irving (2005), NWA 3136 plots in the same compositional fields as MET 01210 based on FeO (wt%) v. CaO (wt %) and FeO (wt%) v. Th (ppm).

While limited chronological context for the 2018–19 DOM clan is currently available, crystallization ages of between 3.86 and 3.96 Ga from DOM 18262 and 18666 are reported in Hayden *et al.* (2022*a*). Within the context of YAMM group chronology, these ages are remarkably similar. From Nyquist *et al.* (2007), the Sm–Nd age for MIL 05025 is 3.80 $\pm$ 0.05 Ga, while the Rb–Sr system yielded 3.90 $\pm$ 0.04 Ga. This is consistent with ages from multiple isotope systems reported by Misawa *et al.* (1993) for A-881757: Pb–Pb, U–Pb and Th–Pb internal isochrons of 3940 $\pm$ 28, 3850 $\pm$ 150 and 3820 $\pm$ 32 Ma in addition to Sm–Nd and Rb–Sr internal isochrons, which yielded 3871 $\pm$ 57 and 3840 $\pm$ 32 Ma, respectively. Collectively, Misawa *et al.* (1993) interpreted a crystallization age for A-881757 of 3.87 Ga with an impact-induced resetting event at 3.8 Ga (as also supported by K–Ar systematics). Similarly, Torigoye-Kita *et al.* (1995) employed a multi-isotope approach to Y-793169 with variable results, ultimately concluding that the concordant 3.8 Ga U–Pb age was representative of a formation age with younger ages indicative of resetting during subsequent thermal events (e.g. a 3.26 Ga Ar–Ar age). For MET 01210, Terada *et al.* (2007) reported a $^{207}Pb/^{206}Pb$–$^{204}Pb/^{206}Pb$ isochron age from merillite and apatite grains in a low-Ti basalt clast, which yielded 3904 $\pm$ 85 Ma, and which is interpreted as a crystallization age (Terada *et al.* 2007). In addition to textural, mineralogical and geochemical similarities, and their crystallization ages, the YAMM group also shares similar cosmic ray exposure histories with ejection ages from the Moon at 0.95 $\pm$ 0.13, 0.80 $\pm$ 0.2 and 0.90 $\pm$ 0.18 Ma for MET 01210, A-881757 and Y-793169, respectively (Thalmann *et al.* 1996; Nishiizumi *et al.* 2006; Arai *et al.* 2010). From the lack of solar-wind-derived components, and the lack of exposure to cosmic rays, it has further been proposed that the YAMM meteorites resided at burial depths greater than a few metres prior to their ejection in a single event ~1 Ma with arrival on Earth as separate falls, <0.05 Ma (Arai *et al.* 2010). Given the mineralogical and compositional (e.g. Fig. 18b, c) and chronological similarities, it is therefore possible

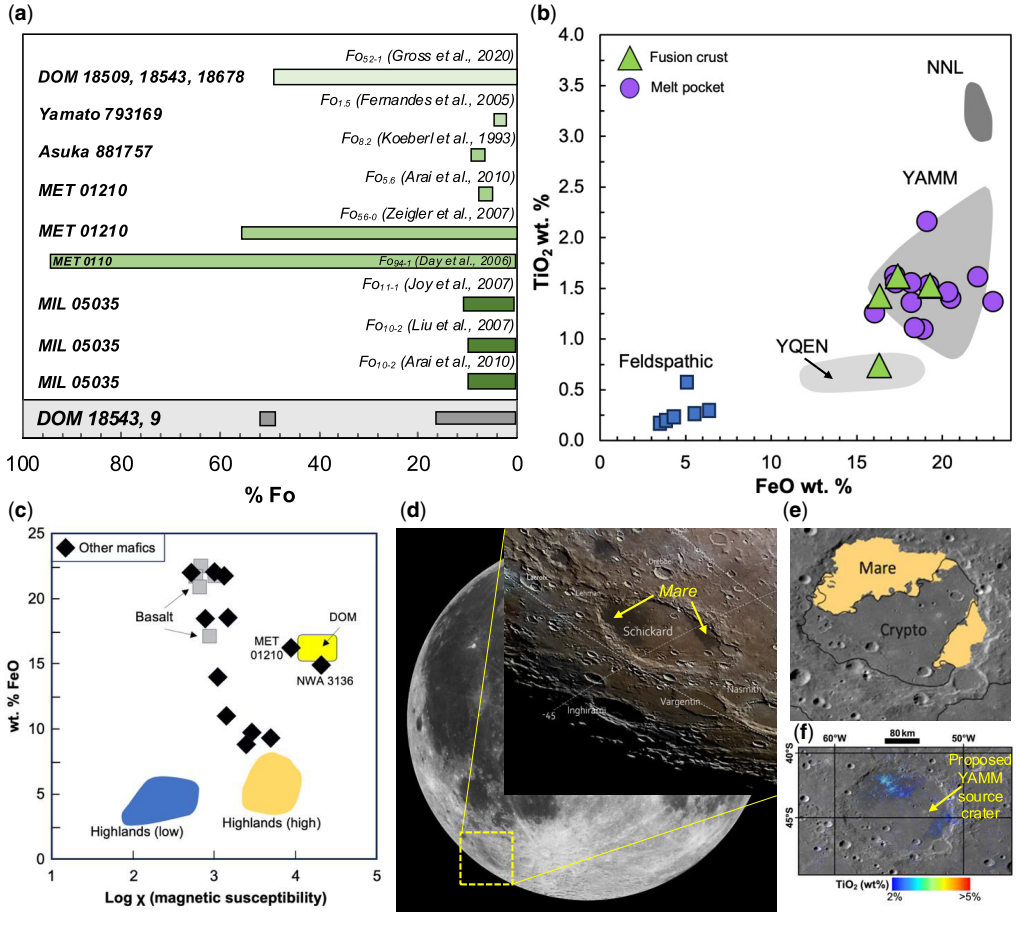


**Fig. 18.** (**a**) DOM 18543,9 olivines compared to YAMM group meteorite olivines. (**b**) FeO v. $TiO_2$ (wt%) for lunar meteorites. Glasses of DOM 18543,9 overlap those of the YAMM suite (glass analyses >24 wt% FeO not shown, see Fig. 13c). YQEN: Yam 793274/981031, EET 87/96, QUE 94281, NWA 4884; YAMM: Yam 793274, Asuka 88175, MET 01210; MIL 05035; NNL: NWA 4734 and NWA 032/479. (**c**) Magnetic susceptibility v. wt% FeO for the 2018–19 lunar DOM meteorites shown in comparison to other lunar meteorites, including NWA 3136 and MET 01210. (**d**) Location of the Schickard crater. Schickard crater is in the centre of the view (~180 km wide), part of the Southern Highlands Lunar Province. Two mare-rich regions are shown. (**e**) Mapped mare and cryptomare units. (**f**) Lunar Reconnaissance Orbiter Camera (LROC) Wide Angle Camera (WAC)-derived $TiO_2$ abundances (wt%) in Schickard crater Source: (a) after Korotev and Zeigler (2014); (c) modified from Righter (2024); (d) image credit: NASA, and Aldo Ferruggia (modified and https licensed under CC BY-SA 4.0: Wikimedia Commons, https://commons.wikimedia.org/wiki/File:Schickard_Si.jpg); (f) from Bramson *et al.* (2022); proposed source crater to the YAMM group associated with the pre-Orientale cryptomare of the Schickard crater after Hawke *et al.* (2006) and Arai *et al.* (2010).

that the lunar DOM 2018–19 suite may be launch-paired with the YAMM group, although no cosmic ray exposure histories are currently available for direct comparison (Gross *et al.* 2020; Zeigler *et al.* 2021; Hayden *et al.* 2022*a*, *b*; Righter 2024).

Within the context of Apollo mare chronology, the launch-paired, KREEP-free, YAMM meteorites (and the aforementioned DOM suite) pre-date the majority of Apollo basaltic magmatism (*c.* 3.8–3.1 Ga) and that of the Chang'e 5 (*c.* 2.0 Ga) and the Chang'e 6 (*c.* 2.8 Ga) basalts (e.g. Jolliff *et al.* 2000; Snape *et al.* 2019; Li *et al.* 2021; Gaffney *et al.* 2023; Shearer *et al.* 2023; Tian *et al.* 2023; Zhang *et al.* 2024; Jin *et al.* 2025; Su *et al.* 2025). Of note, however, from the Apollo record are the relatively old ages of high-Ti, Apollo 11 Group B basalt 10003, which has yielded ages of *c.* 3.8–3.9 Ga from multiple isotope systems (Snape *et al.* 2019).

Furthermore, the basaltic clasts of the YAMM group are recognized to be distinct from Apollo and Luna basalts with lower Ti/Fe ratios, low μ $^{238}U/^{206}Pb$ values (μ: 9–20), and with more extensive fractionation from a mantle source more depleted than that of the low-Ti Apollo 12 and 15 basalts, possibly from early lunar magma ocean olivine–orthopyroxene cumulates (Jolliff *et al.* 1993, 2000; Torigoye-Kita *et al.* 1995; Day *et al.* 2006; Joy *et al.* 2008). More recent work by Srivastava *et al.* (2024) focusing on A-881757 proposed a relatively shallow lunar mantle origin for the YAMM source magmas (~60–100 km). Melts derived from this source subsequently experienced polybaric crystallization and were emplaced as cryptomare. Within these contexts, several potential source regions on the lunar surface have been proposed, one of which is an unnamed 1.4 km-diameter crater associated with cryptomare in the Schickard crater region summarized in Figure 18c–e, as first proposed in Arai *et al.* (2010). This was subsequently suggested as a potential location for the 2018–19 lunar DOM clan by Hayden *et al.* (2022*a*). The floor of this crater contains both dark (mare) and light deposits with FeO values ranging from 11.4 to 15.3 wt% and $TiO_2$ values ranging from 0.4 to 3.0 wt%, and is covered in Mare Orientale (and more local) ejecta (Blewett *et al.* 1995; Hawke *et al.* 2006; Arai *et al.* 2010). With respect to mare basalt ages in this region, the buried basalts are proposed as Imbrian or older in age with material excavated from a pre-Nectarian crater in at least one dark holed crater with post-Orientale basalts also present (0.4–2.6 wt% $TiO_2$; Hawke *et al.* 2006). From Arai *et al.* (2010), the reported FeO, $TiO_2$ and Th contents, the presence of feldspathic materials, the occurrence of pre-Orientale cryptomare (older than 3.8 Ga), and immaturity of ejecta material around the unnamed crater (<2 Ma) were all taken to support this as the location of origin of the YAMM groups. However, other points of origin for the YAMM group have also been proposed by several authors, including: (1) Mare Cognitum on the basis of Ti/Fe ratios (Jolliff *et al.* 1993); (2) Mare Crisium and Fecunditatis on the basis of the low-Ti signatures and relatively low FeO contents (8.2–8.6 wt%) based on Lunar Prospector data, although it is noted that the basalts in those regions may also be too young to account for the YAMM group (3.5–3.7 Ga; Joy *et al.* 2010); and (3) Mare Crism for MET 01210 and Mare Fecunditatis for Y-793169, A-881757 and MIL 05035 on the basis of overlapping regolith compositions and late Imbrian crystallization ages (see fig. 3 of Calzada-Diaz *et al.* 2015). In each case, the availability of mare, feldspathic and regolith materials, in conjunction with the local chronological framework, is consistent with the features of the YAMM and 2018–19 lunar DOM clan.

Future studies of the YAMM and DOM meteorites should therefore be coordinated and work to complement each other to determine whether they are launch-paired. For DOM samples, acquisition of cosmic ray exposure ages and assessment of solar-wind components should be completed, in addition to multi-isotope geochronology to evaluate crystallization and magmatic histories. Textural, mineralogical and geochemical characterization of the entire 2018–19 lunar DOM clan should be completed to further confirm the pairings. All sample-based data should be integrated with available remote sensing datasets to further evaluate potential source regions from the lunar near and farside.

## Conclusions

Lunar meteorites provide critical insights into the Moon's geological evolution and extend our understanding of differentiated planetary bodies in the Solar System. During the 2018–19 ANSMET, eight basaltic, polymict regolith breccias were recovered from the Dominion Range, and represent the first ANSMET lunar finds since 2001. This study focuses on thin section −9 of DOM 18543.

The DOM 18543,9 meteorite is clast-poor (<10%), containing basalts, gabbros, impact melt breccias and three-phase symplectites in addition to one FAN-dominated (anorthositic granulite) microbreccia clast. All clasts are embedded within a glassy matrix. Mineral fragments include clinopyroxene, plagioclase and olivine, with accessory Fe–Ti oxides, sulfides and phosphates. The studied section is ~75% rimmed by a vesiculated, glassy fusion crust. Notable features include melt veins (up to 80 μm wide), abundant glass spherules (up to 400 μm), and symplectites comprising Fe-rich olivine, clinopyroxene and silica. EPMA reveals that pyroxenes range from augite to pigeonite compositions. Orthopyroxenes are rare. Olivines are dominantly fayalitic ($Fa_{85.0–98.7}$), with only two magnesian grains ($Fa_{49.5,Fa36.1}$). Plagioclase feldspars are mostly anorthitic ($An_{92.9–99.2}$), with a few bytownitic grains ($An_{85.8–89.1}$). Plagioclase compositions within the FAN-dominated microbreccia clast are tightly constrained to $An_{96–97}$. Fe/Mn ratios in pyroxenes (avg. 0.015 ± 0.005) and olivines (avg. 0.012 ± 0.002) confirm its lunar provenance.

The major element chemistry of DOM 18543,9 pyroxene, ilmenite and olivine is consistent with derivation from a compositionally evolved, low-Ti basalt that represents late-stage fractionation. This feature is shared by several of the basaltic components in the YAMM meteorite group, which also share similarities in bulk composition and chronology. This DOM clan is therefore potentially paired with the YAMM group with collective derivation

from an ancient, basaltic, KREEP-poor lava flow on the lunar surface where feldspathic material is available locally. While an unnamed crater within the Schickard crater on the Moon's southwestern nearside has been proposed as one such location for the YAMM group, further characterization of the DOM clan is needed. This includes cosmic ray exposure data, complete characterization of all eight meteorites, a coordinated, multi-isotopic investigation of clast types within both the DOM and the YAMM groups, and integration of remote sensing data. This would contribute to a better petrological framework in which their potential paired relationship could be evaluated, and advance our understanding of locations on the Moon from which meteoritic material is derived.

**Acknowledgements** US Antarctic meteorite samples are recovered by the Antarctic Search for Meteorites (ANSMET) programme, and characterized and curated by the Department of Mineral Sciences of the Smithsonian Institution and Astromaterials Curation Office at NASA Johnson Space Center. The study of meteorite DOM 18543,9 was supported by Meteorite Working Group request #3625 (PI: McLeod; co-PI: Shaulis). Thanks are extended to Matt Duley at the Miami University Center for Advanced Microscopy and Imaging (CAMI) for guidance and training during SEM-EDS data collection. The authors extend sincere thanks to Minako Righter and Tara Hayden, and to editor Thomas Barrett, for providing constructive, thought-provoking comments on earlier drafts of this work. Changes made as a result of their guidance improved the manuscript.

**Competing interests** The authors declare that they have no known competing financial interests or personal relationships that could have appeared to influence the work reported in this paper.

**Author contributions** **ASc**: formal analysis (lead), investigation (lead), methodology (lead), visualization (equal), writing – original draft (lead), writing – review & editing (equal); **CLM**: formal analysis (supporting), investigation (supporting), methodology (supporting), project administration (lead), supervision (lead), visualization (supporting), writing – review & editing (supporting); **AJG**: formal analysis (supporting), investigation (supporting), supervision (supporting), visualization (supporting), writing – review & editing (supporting); **ASe**: data curation (supporting), formal analysis (supporting), visualization (supporting), writing – review & editing (supporting); **MLL**: formal analysis (supporting), project administration (supporting), supervision (supporting), writing – review & editing (supporting); **BS**: conceptualization (supporting), methodology (supporting), project administration (supporting), writing – review & editing (supporting); **ML**: conceptualization (supporting), formal analysis (supporting), methodology (supporting), writing – review & editing (supporting).

**Funding** The ANSMET programme has been funded by NSF and NASA. The Miami University Graduate School is acknowledged for providing financial support in the form of travel funding that supported the presentation of preliminary findings from this work to author ASc. Throughout this work, ASc and ASe were supported by Graduate Teaching Assistantships from the Department of Geology and Environmental Earth Science at Miami University and were the recipients of summer research fellowships from the Miami University Graduate School. AJG acknowledges support from Future Investigators in NASA Earth and Space Science and Technology (FINESST) award #80NSSC22K1371 during this work.

**Data availability** All data generated or analysed during this study are included in this published article and, if present, its supplementary information files.

## References

Anand, M., Taylor, L.A., Floss, C., Neal, C.R., Terada, K. and Tanikawa, S. 2006. Petrology and geochemistry of LaPaz Icefield 02205: a new unique low-Ti mare-basalt meteorite. *Geochimica et Cosmochimica Acta*, **70**, 246–264, https://doi.org/10.1016/j.gca.2005.08.018

Arai, T., Takeda, H. and Warren, P.H. 1996. Four lunar meteorites: crystallization trends of pyroxenes and spinels. *Earth and Planetary Science*, **31**, 877–892, https://doi.org/10.1111/j.1945-5100.1996.tb02121.x

Arai, T., Hawke, B.R., Giguere, T.A., Misawa, K., Miyamoto, M. and Kojima, H. 2010. Antarctic lunar meteorites Yamato-793169, Asuka-881757, MIL 05035, and MET 01210 (YAMM): Launch pairing and possible cryptomare origin. *Geochimica et Cosmochimica Acta*, **74**, 2231–2248, https://doi.org/10.1016/j.gca.2009.11.019

Atkinson, N. 2010. Is the Moon Really a 'Been There Done That' World? *Universe Today*, https://www.universetoday.com/69505/is-the-moon-really-a-been-there-done-that-world/ [last accessed 6 June 2025]

Baars, J.W.M. and Kärcher, H.J. 2018. Evolution of the telescope. *In*: *Radio Telescope Reflectors. Astrophysics and Space Science Library*. Springer, Cham, 447, https://doi.org/10.1007/978-3-319-65148-4_2

Barrett, T.J., Robinson, K.L. *et al*. 2023. Deciphering the origin(s) of H and Cl in Apollo 15 quartz monzodiorites: evidence for multiple processes and reservoirs. *Geochimica et Cosmochimica Acta*, **358**, 192–206, https://doi.org/10.1016/j.gca.2023.08.004

Basilevsky, A.T. and Head, J.W., III. 1998. The geologic history of Venus: a stratigraphic view. *Journal of Geophysical Research Planets*, **103**, 8531–8544, https://doi.org/10.1029/98JE00487

Bicknell, P.J. 1969. Anaximenes' Astronomy. *Acta Classica*, **12**, 53.85. Available online, https://journals.co.za/doi/pdf/10.10520/AJA00651141_855 [last accessed 4 June 2025]

Blewett, D.T., Hawke, B.R., Lucey, P.G., Taylor, G.J., Jaumann, R. and Spudis, P.D. 1995. Remote sensing and geologic studies of the Schiller-Schickard region of the Moon. *Journal of Geophysical Research: Planets*,

**100**, 16959–16977, https://doi.org/10.1029/95JE01409

Bouvier, A., Blichert-Toft, J. and Albarède, F. 2009. Martian meteorite chronology and the evolution of the interior of Mars. *Earth and Planetary Science Letters*, **280**, 285–295, https://doi.org/10.1016/j.epsl.2009.01.042

Bramson, A.M., Carter, L.M. *et al*. 2022. Burial depths of extensive shallow cryptomaria in the lunar Schiller–Schickard region. *The Planetary Science Journal*, **3**, 216, https://doi.org/10.3847/PSJ/ac8670

Breuer, D., Hauck, S.A., Buske, M., Pauer, M. and Spohn, T. 2007. Interior evolution of Mercury. *Space Science Reviews*, **132**, 229–260, https://doi.org/10.1007/s11214-007-9228-9

Calzada-Diaz, A., Joy, K.H., Crawford, I.A. and Nordheim, T.A. 2015. Constraining the source regions of lunar meteorites using orbital geochemical data. *Meteoritics & Planetary Science*, **50**, 214–228, https://doi.org/10.1111/maps.12412

Cambioni, S., Jacobson, S.A. *et al*. 2021. The effect of inefficient accretion on planetary differentiation. *The Planetary Science Journal*, **2**, 93, https://doi.org/10.3847/PSJ/abf0ad

Canup, R.M. 2012. Forming a moon with an earth-like composition via a giant impact. *Science*, **338**, 1052–1055, https://doi.org/10.1126/science.1226073

Canup, R.M., Visscher, C., Salmon, J. and Fegley, B., Jr 2015. Lunar volatile depletion due to incomplete accretion within an impact-generated disk. *Nature Geoscience*, **8**, 918–921, https://doi.org/10.1038/ngeo2574

Carr, M.H. and Head, J.W., III 2010. Geologic history of Mars. *Earth and Planetary Science Letters*, **294**, 185–203, https://doi.org/10.1016/j.epsl.2009.06.042

Chauhan, P., Kaur, P., Srivastava, N., Sinha, R.K., Jain, N. and Murty, S.V.S. 2015. Hyperspectral remote sensing of planetary surfaces: an insight into composition of inner planets and small bodies in the solar system. *Current Science*, **108**, 915–924, https://www.jstor.org/stable/24216520

Che, X., Nemchin, A. *et al*. 2021. Age and composition of young basalts on the Moon, measured from samples returned by Chang'e-5. *Science*, **374**, 887–890, https://doi.org/10.1126/science.abl7957

Che, X., Long, T. *et al*. 2025. Isotopic and compositional constraints on the source of basalt collected from the lunar farside. *Science*, **387**, 1306–1310, https://doi.org/10.1126/science.adt3332

Cui, Z., Yang, Q. *et al*. 2024. A sample of the Moon's far side retrieved by Chang'e-6 contains 2.83-billion-year-old basalt. *Science*, **386**, 1395–1399, https://doi.org/10.1126/science.adt1093

Curran, N.M., Joy, K.H. *et al*. 2019. The early geological history of the Moon inferred from ancient lunar meteorite Miller Range 13317. *Meteoritics & Planetary Science*, **54**, 1401–1430, https://doi.org/10.1111/maps.13295

Day, J.M.D., Floss, C., Taylor, L.A., Anand, M. and Patchen, A.D. 2006. Evolved mare basalt magmatism, high Mg/Fe feldspathic crust, chondritic impactors, and the petrogenesis of Antarctic lunar breccia meteorites Meteorite Hills 01210 and Pecora Escarpment 02007. *Geochimica et Cosmochimica Acta*, **70**, 5957–5989, https://doi.org/10.1016/j.gca.2006.05.001

Des Marais, D.J., Harwit, M.O. *et al*. 2004. Remote sensing of planetary properties and biosignatures on extrasolar terrestrial planets. *Astrobiology*, **2**, https://doi.org/10.1089/15311070260192246

Donohue, P.H. and Neal, C.R. 2018. Textural and mineral chemical evidence for the cumulate origin and evolution of high-titanium basalt fragment 71597. *American Mineralogist*, **103**, 284–297, https://doi.org/10.2138/am-2018-6173

Du, W. and Yang, J. 2024. The Moon's early magmatic activities: from the perspective of lunar alkali-suite and Mg-suite samples. *Space: Science & Technology*, **4**, 0118, https://doi.org/10.34133/space.0118

El Goresy, A. 1976. Oxide minerals in lunar rocks. *In*: Rumble, D. (ed.) *Oxide Minerals*. Mineralogical Society of America, De Gruyter, https://doi.org/10.1515/9781501508561-010

Eugster, O. 1989. History of Meteorites from the Moon collected in Antarctica. *Science*, **245**, 1197–1202, https://doi.org/10.1126/science.245.4923.1197

Fernandes, V.A., Burgess, R. and Morris, A. 2009. $^{40}$Ar-$^{39}$Ar age determinations of lunar basalt meteorites Asuka 881757, Yamato 793169, Miller Range 05035, La Paz Icefield 02205, Northwest Africa 479, and basaltic breccia Elephant Moraine 96008. *Meteoritics & Planetary Science*, **44**, 805–821, https://doi.org/10.1111/j.1945-5100.2009.tb00770.x

Gaffney, A.M., Gross, J. *et al*. 2023. Magmatic evolution I: initial differentiation of the moon. *Reviews in Mineralogy & Geochemistry*, 89, https://doi.org/10.2138/rmg.2023.89.03

Gattacceca, J., McCubbin, F.M., Bouvier, A. and Grossman, J.N. 2020. The Meteoritical Bulletin, No. 108. *Meteoritics & Planetary Science*, **55**, 1146–1150, https://doi.org/10.1111/maps.13493

Ghail, R.C., Smrekar, S.E. *et al*. 2024. Volcanic and tectonic constraints on the evolution of Venus. *Space Science Reviews*, **220**, 36, https://doi.org/10.1007/s11214-024-01065-2

Giguere, T.A., Taylor, G.J., Hawke, B.R. and Lucey, P.G. 2000. The titanium contents of lunar mare basalts. *Meteoritics & Planetary Science*, **35**, 193–200, https://doi.org/10.1111/j.1945-5100.2000.tb01985.x

Gross, J., Eckley, S., Zeigler, R.A. and Vander Kaaden, K.E. 2020. Treasure Trove Antarctica: Petrology, Geochemistry and Pairing of Lunar Meteorites Dominion Range (DOM) 18509, 18543, and 18678. 51st Lunar and Planetary Science Conference, The Woodlands, TX. 16–20 March, abstract #2555, https://www.hou.usra.edu/meetings/lpsc2020/pdf/2555.pdf

Grove, T.L. and Beaty, D.W. 1980. Classification, experimental petrology and possible volcanic histories of the Apollo 11 high-K basalts. Proceedings of the 11th Lunar and Planetary Science Conference, Houston, TX, 17–21 March. Volume 1. (A82-22251 09-91), Pergamon Press, New York, 149–177.

Gugino, J., McLeod, C.L., Sedaghat, A., Schweitzer, A.R. and Shaulis, B. 2024*a*. Insights into the lunar impact glass record from Dominion (DOM) Range lunar meteorites DOM 18543 and 18666. 55th Lunar and Planetary Science Conference, 11–15 March, The Woodlands, TX, https://www.hou.usra.edu/meetings/lpsc2024/pdf/2049.pdf

Gugino, J., McLeod, C.L., Sedaghat, A., Schweitzer, A. and Shaulis, B. 2024*b*. Petrography and chemistry of lunar impact glasses from Dominion (DOM) Range

lunar meteorites DOM 18543 and 18666: constraining lunar geology and impact flux. Joint 58th Annual North-Central/58th Annual South-Central Section Meeting, Springfield, MO, 21–23 April, https://gsa.confex.com/gsa/2024NC/meetingapp.cgi/Paper/398902

Haloda, J., Týcová, P. *et al*. 2009. Petrology, geochemistry, and age of low-Ti mare-basalt meteorite Northeast Africa 003-A: a possible member of the Apollo 15 mare basaltic suite. *Geochimica et Cosmochica Acta*, **73**, 3450–3470, https://doi.org/10.1016/j.gca.2009.03.003

Harvey, R.P. 2003. The origin and significance of Antarctic meteorites. *Geochemistry*, **63**, 93–147, https://doi.org/10.1078/0009-2819-00031

Haskin, L. and Warren, P. 1991. Lunar chemistry. *In*: Heiken, G.H., Vaniman, D.R. and French, B.M. (eds) *Lunar Sourcebook*. Cambridge University Press, available online, https://www.lpi.usra.edu/publications/books/lunar_sourcebook/ [accessed 25 July 2025]

Hauck, S.A., II, Dombard, A.J., Phillips, R.J. and Solomon, S.C. 2004. Internal and tectonic evolution of Mercury. *Earth and Planetary Science Letters*, **222**, 713–728, https://doi.org/10.1016/j.epsl.2004.03.037

Hawke, B.R., Giguere, T.A. *et al*. 2006. Ancient volcanism in the Schiller–Schickard region of the Moon. 37th Lunar and Planetary Science Conference, The Woodlands, TX, 13–17 March, abstract #1516, https://www.lpi.usra.edu/meetings/lpsc2006/pdf/1516.pdf

Hayden, T.S. 2023. *Assessing the volatile inventory and history of the Moon using lunar meteorites*. PhD thesis, The Open University, https://doi.org/10.21954/ou.ro.0001569f

Hayden, T.S., Barrett, T.J., Zhao, X., Degli-Alessandrini, G., Anand, M. and Franchi, A. 2021. Chlorine and hydrogen in brecciated lunar meteorites: implications for lunar volatile history. 52nd Lunar and Planetary Science Conference, The Woodlands, TX, 15–19 March, abstract #1550, https://www.hou.usra.edu/meetings/lpsc2021/pdf/1550.pdf

Hayden, T.S., Barrett, T.J., Whitehouse, M.J., Jeon, H., Zhao, X., Anand, M. and Franchi, I.A. 2022*a*. Mineralogy, geochemistry, and geochronology of lunar meteorites from the Dominion Range, and their pairing relationships. 53rd Lunar and Planetary Science Conference, The Woodlands, TX, 7–11 March, abstract #1894, https://www.hou.usra.edu/meetings/lpsc2022/pdf/1894.pdf

Hayden, T., Barrett, T., Zhao, X., Anand, M. and Franchi, I. 2022*b*. Volatile inventory of lunar meteorites from the Dominion Range. 53rd Lunar and Planetary Science Conference, The Woodlands, TX, 7–11 March, abstract #1886, https://www.hou.usra.edu/meetings/lpsc2022/pdf/1886.pdf

Heiken, G.H., Vaniman, D.T. and French, B.M. 1991. *Lunar Sourcebook: A User's Guide to the Moon*. Cambridge University Press, available online, https://www.lpi.usra.edu/publications/books/lunar_sourcebook/ [accessed 4 June 2025]

Hiesinger, H., Marchi, S. *et al*. 2016. Cratering on Ceres: implications for its crust and evolution. *Science*, **353**, https://doi.org/10.1126/science.aaf4759

Howat, I.M., Porter, C., Smith, B.E., Noh, M.-J. and Morin, P. 2019. The reference elevation model of Antarctica. *The Cryosphere*, **13**, 665–674, https://doi.org/10.5194/tc-13-665-2019

Huber, H. and Warren, P.H. 2005. MET01210: another lunar mare meteorite (regolith breccia) with extensive pyroxene exsolution and not part of the YQ Launch Pair. 36th Lunar and Planetary Science Conference, The Woodlands, TX, 14–18 March, abstract #2401, https://www.lpi.usra.edu/meetings/lpsc2005/pdf/2401.pdf

James, O.B., Lindstrom, M.M. and Flohr, M.F. 1987. Petrology and geochemistry of alkali gabbronorites from lunar breccia 67975. *Journal of Geophysical Research*, **92**, E314–E330, https://doi.org/10.1029/JB092iB04p0E314

Jin, Z., Hou, T., Zhu, M.-H., Zhang, Y. and Namur, O. 2025. Late-stage microstructures in Chang'E-5 basalt and implications for the evolution of lunar ferrobasalt. *American Mineralogist*, **110**, 560–569, https://doi.org/10.2138/am-2024-9448

Jolliff, B. and Robinson, M.S. 2019. The scientific legacy of the Apollo program. *Physics Today*, **72**, 44–50, https://doi.org/10.1063/PT.3.4249

Jolliff, B.L., Korotev, R.L. and Haskin, L.A. 1993. Lunar basaltic meteorites Yamato-793169 and Asuka-881757: Samples of the same low-Ti mare-lava? Papers Presented to the Eighteenth Symposium on Antarctic Meteorites, National Institute of Polar Research, Tokyo, 31 May–2 June, 214–217, https://epsc.wustl.edu/~rlk/papers/jolliff_et_al_1993_nipr_asuka-881757_&_yamato-793169.pdf

Jolliff, B.L., Gillis, J.J., Haskin, L.A., Korotev, R.L. and Wieczorek, M.A. 2000. Major lunar crustal terranes: surface expressions and crust-mantle origins. *Journal of Geophysical Research: Planets*, **105**, 4197–4216, https://doi.org/10.1029/1999JE001103

Joy, K. H. and Crawford, I. A. 2006. Lunar meteorite regolith breccias MET 01210, DaG 400 and PCA02007: Their geochemistry and importance in understanding the nature of the lunar surface. *Geophysical Research Abstracts*, **8**, 00732, https://meetings.copernicus.org/www.cosis.net/abstracts/EGU06/00732/EGU06-J-00732.pdf

Joy, K.H., Crawford, I.A., Anand, M., Greenwood, R.C., Franchi, I.A. and Russell, S.S. 2008. The petrology and geochemistry of Miller Range 05035: a new lunar gabbroic meteorite. *Geochimica et Cosmochimica Acta*, **72**, 3822–3844, https://doi.org/10.1016/j.gca.2008.04.032

Joy, K.H., Crawford, I.A., Russell, S.S. and Kearsley, A.T. 2010. Lunar meteorite regolith breccias: an in situ study of impact melt composition using LA-ICP-MS with implications for the composition of the lunar crust. *Meteoritics & Planetary Science*, **45**, 917–946, https://doi.org/10.1111/j.1945-5100.2010.01067.x

Joy, K., Barnes, J.J., Che, X. and Jolliff, B. 2025. It's not just a phase: over 50 years of lunar sample science. *Elements*, **21**, 327–332, https://doi.org/10.2138/gselements.21.5.327

Karner, J., Papike, J.J. and Shearer, C.K. 2006. Comparative planetary mineralogy: pyroxene major- and minor-element chemistry and partitioning of vanadium between pyroxene and melt in planetary basalts. *American Mineralogist*, **91**, 1574–1582, https://doi.org/10.2138/am.2006.2103

Ketchum, R.A. 2015. Technical Note: Calculation of stoichiometry from EMP data for apatite and other phases

with mixing on monovalent anion sites. *American Mineralogist*, **100**, 1620–1623, , https://doi.org/10.2138/am-2015-5171

Kim, J., Lin, S.-Y. and Xiao, H. 2023. Remote sensing and data analyses on planetary topography. *Remote Sensing*, **15**, 2954, https://doi.org/10.3390/rs15122954

Koeberl, C., Kurat, G. and Brandstätter, F. 1993. Gabbroic lunar mare meteorites Asuka-881757 (Asuka-31) and Yamato-793169: geochemical and mineralogical study. Seventeenth Symposium on Antarctic Meteorites, Proceedings of the NIPR Symposium, National Institute of Polar Research, Tokyo, 19–21 August, No. 6.

Korotev, R.L. 2005. Lunar geochemistry as told by lunar meteorites. *Geochemistry*, **65**, 297–346, https://doi.org/10.1016/j.chemer.2005.07.001

Korotev, R.L. 2025*a*. Lunar Meteorites-Some Meteorite Information-Washington University in St. Louis, https://www.sites.wustl.edu/meteoritesite/items/lunar-meteorites [last accessed 6 June 2025]

Korotev, R.L. 2025*b*. Some Meteorite Information - Meteorite statistics. Available online, https://sites.wustl.edu/meteoritesite/items/some-meteorite-statistics/ [last accessed 4 June 2025]

Korotev, R.L. and Irving, A.J. 2005. Compositions of three lunar meteorites: Meteorite Hills 01210, Northeast Africa 001; and Northwest Africa 3136. 36th Lunar and Planetary Science Conference, The Woodlands, TX, 14–18 March, abstract #1220, https://www.lpi.usra.edu/meetings/lpsc2005/pdf/1220.pdf

Korotev, R. L. and Zeigler, R. A. 2014. ANSMET Meteorites from the Moon. In: Righter, K., Corrigan, C. M., McCoy, T. and Harvey, R. P. (eds) *35 Seasons of U.S. Antarctic Meteorites (1976–2010): A Pictorial Guide to the Collection*, Special Publication **68**, John Wiley & Sons, Inc, https://doi.org/10.1002/9781118798478.ch6

Korotev, R. L., Zeigler, R. A., Jolliff, B. L., Irving, A. J. and Bunch, T. E. 2009. Compositional and lithological diversity among brecciated lunar meteorites of intermediate iron concentration. *Meteoritics & Planetary Science*, **44**, 1287–1322, https://doi.org/10.1111/j.1945-5100.2009.tb01223.x

Kuehner, S.M., Irving, A.J., Rumble, D., III, Hupé, A.C. and Hupé, G.M. 2005. Mineralogy and petrology of lunar meteorite NWA 3136: a glass-welded mare regolith breccia of mixed heritage. 36th Lunar and Planetary Science Conference, The Woodlands, TX, 14–18 March, abstract #1228, https://www.lpi.usra.edu/meetings/lpsc2005/pdf/1228.pdf

Laneuville, M., Taylor, J. and Wieczorek, M.A. 2018. Distribution of radioactive heat sources and thermal history of the moon. *Journal of Geophysical Research Planets*, **123**, 3144–3166, https://doi.org/10.1029/2018JE005742

Li, C., Hu, H. *et al*. 2022. Characteristics of the lunar samples returned by the Chang'E-5 mission. *National Science Review*, **9**, nwab188, https://doi.org/10.1093/nsr/nwab188

Li, C., Hu, H. *et al*. 2024. Nature of the lunar far-side samples returned by the Chang'E-6 mission. *National Science Review*, **11**, nwae328, https://doi.org/10.1093/nsr/nwae328

Li, Q.-L., Zhou, Q. *et al*. 2021. Two-billion-year-old volcanism on the Moon from Chang'e-5 basalts. *Nature*, **600**, 54–58, https://doi.org/10.1038/s41586-021-04100-2

Li, S., Zhang, D. *et al*. 2024. An anorthositic meteorite supporting an ancient magma ocean on Vesta. *Nature Astronomy*, **8**, 739–747, https://doi.org/10.1038/s41550-024-02243-6

Lindstrom, M.M. and Lindstrom, D.J. 1986. Lunar granulites and their precursor anorthositic norites of the early lunar crust. *Journal of Geophysical Research*, **91**, D263–D276, https://doi.org/10.1029/JB091iB04p0D263

McCubbin, F.M., Jolliff, B.L. *et al*. 2011. Fluorine and chlorine abundances in lunar apatite: implications for heterogeneous distributions of magmatic volatiles in the lunar interior. *Geochimica et Cosmochimica Acta*, **75**, 5073–5093, https://doi.org/10.1016/j.gca.2011.06.017

McLeod, C.L. and Sedaghat, A. 2025. Insights into planetary processes from enigmatic 3-phase symplectites (olivine-clinopyroxene-silica) in basaltic lunar breccias. Joint 59th annual North-Central/60th annual Northeastern Geological Society of America Section Meeting, Erie, PA, 27–30 March, https://gsa.confex.com/gsa/2025NE/webprogram/Paper408880.html

McLeod, C.L., Shaulis, B., Brum, J.T. and Gawronska, A.J. 2020. More meteorites, more insights! Five new lunar basaltic meteorites from the Dominion Range. 51st Lunar and Planetary Science Conference, The Woodlands, TX, 16–20 March, abstract #2326, https://www.hou.usra.edu/meetings/lpsc2020/pdf/2634.pdf

McLeod, C.L., Shaulis, B., Gawronska, A., Schweitzer, A. and Loocke, M. 2024. Meteorite forensics: petrological and geochemical characterization of lunar meteorite Dominion Range (DOM) Range 18666. Geological Society of America Annual Meeting, San Antonio, TX, 22–25 September, https://gsa.confex.com/gsa/2024AM/meetingapp.cgi/Paper/401532

McSween, H.Y., Jr, Raymond, C.A. *et al*. 2019. Differentiation and magmatic history of Vesta: constraints from HED meteorites and Dawn spacecraft data. *Geochemistry*, **79**, 125526, https://doi.org/10.1016/j.chemer.2019.07.008

Misawa, K., Tatsumoto, M., Dalrymple, G.B. and Yanai, K. 1993. An extremely low U/Pb source in the Moon: U–Th–Pb, Sm–Nd, Rb–Sr, and $^{40}Ar/^{39}Ar$ isotopic systematics and age of lunar meteorite Asuka 881757. *Geochimica et Cosmochimica Acta*, **56**, 4687–4702, https://doi.org/10.1016/0016-7037(93)90193-Z

NASA. 2023. Lunar Rocks and Soils from Apollo Missions. Available online, https://www-curator.jsc.nasa.gov/lunar/index.cfm [last accessed 4 June 2025]

Nishiizumi, K., Hillegonds, D.J. and Welten, K.C. 2006. Exposure and terrestrial histories of lunar meteorites LaP 02205/02224/02226/02436, MET 01210, and PCA 02007. 37th Lunar and Planetary Science Conference, The Woodlands, TX, 13–17 March, abstract #2369, https://www.lpi.usra.edu/meetings/lpsc2006/pdf/2369.pdf

Norman, M. 2005. Lunar impact breccias: petrology, crater setting, and bombardment history of the Moon. *Australian Journal of Earth Sciences*, **52**, 711–723, https://doi.org/10.1080/08120090500170443

Nyquist, L.E., Shih, C.-Y. and Reese, Y.D. 2007. Sm-Nd and Rb-Sr ages for MIL 05035: implications for surface and mantle sources. 38th Lunar and Planetary Science Conference, The Woodlands, TX, 16–20 March, abstract #1702, https://ntrs.nasa.gov/api/citations/20070003760/downloads/20070003760.pdf

O'Donnell, S. P., Jolliff, B. L., Zeigler, R. A. and Korotev, R. L. 2008. Identifying the Mafic Components in Lunar Regolith Breccia NWA 3136. *39th Lunar and Planetary Science Conference*, #2507, https://www.lpi.usra.edu/meetings/lpsc2008/pdf/2507.pdf

Oliveira, B.H., Snape, J.F., Tartèse, R., Jeon, H., Whitehouse, M.J. and Joy, K.H. 2025. A petrological, geochemical, and geochronological study of Ramlat Fasad 532: an Omani addition to the Antarctic 'YAMM' lunar meteorite group. *Advances in Geochemistry and Cosmochemistry*, **1**, 772, https://doi.org/10.33063/agc.v1i2.772

Osinski, G.R., Grieve, R.A.F. *et al*. 2025. A proposed new classification scheme and nomenclature for impactites from the Earth and Moon. 56th Lunar and Planetary Science Conference, The Woodlands, TX, 10–14 March, abstract #1765, https://www.hou.usra.edu/meetings/lpsc2025/pdf/1765.pdf

Papike, J.J., Hodges, F.N., Bence, A.E., Cameroni, R.M. and Rhodes, J.M. 1976. Mare basalts–crystal chemistry, mineralogy, and petrology. *Reviews of Geophysics*, **14**, 475–540, https://doi.org/10.1029/RG014i004p00475

Papike, J.J., Taylor, L.A. and Simon, S.B. 1991. Lunar minerals. *In*: Heiken, G.H., Vaniman, D.T. and French, B.M. (eds) *Lunar Sourcebook: A User's Guide to the Moon*. Cambridge University Press, 121–181.

Papike, J.J., Karner, J.M. and Shearer, C.K. 2003. Determination of planetary basalt parentage: a simple technique using the electron microprobe. *American Mineralogist*, **88**, 469–472, https://doi.org/10.2138/am-2003-2-323

Pernet-Fisher, J.F., Joy, K.H., Martin, D.J.P. and Donaldson Hanna, K.L. 2017. Assessing the shock stage of the lunar highlands: implications for the petrogenesis and chronology of crustal anorthosites. *Nature Scientific Reports*, **7**, 5888, https://doi.org/10.1038/s41598-017-06134-x

Pernet-Fisher, J.F., McDonald, F.E., Zeigler, R.A. and Joy, K.H. 2019. 50 years on: legacies of the Apollo programme. *Astronomy & Geophysics*, **60**, 4.22–4.28, https://doi.org/10.1093/astrogeo/atz163

Polar Geospatial Center. 2019. *REMA: Reference Elevation Model of Antarctica, Version 1*. University of Minnesota, https://doi.org/10.7910/DVN/SAIK8B

Potts, N.J., Tartèse, R., Anand, M., van Westrenen, W., Griffiths, A.A., Barrett, T.J. and Franchi, I.A. 2016. Characterization of mesostasis regions in lunar basalts: understanding late-stage melt evolution and its influence on apatite formation. *Meteoritics & Planetary Science*, **51**, 1555–1575, https://doi.org/10.1111/maps.12681

Righter, K. 2024. Lunar sample compendium; Dominion Range 18242, 18244, 18262, 18509, 18543, 18545, 18666, 18678. Available online, https://curator.jsc.nasa.gov/antmet/PDFFiles/DOM18242.pdf [last accessed 7 June 2025]

Righter, K., Schutt, C. *et al*. 2023. The Dominion Range (DOM) Lunar Regolith Breccia Pairing Group. 54th Lunar and Planetary Science Conference, The Woodlands, TX, 13–17 March, abstract #2109, https://ntrs.nasa.gov/api/citations/20230000336/downloads/LPSC-23-DOM-lunars-2-2109.pdf [last accessed 4 June 2025]

Roberts, S.E., McCanta, M.C., Jean, M.M. and Taylor, L.A. 2019. New lunar meteorite NWA 10986: a mingled impact melt breccia from the highlands – a complete cross section of the lunar crust. *Meteoritics & Planetary Science*, **54**, 3018–3035, https://doi.org/10.1111/maps.13406

Robinson, K.L., Treiman, A.H. and Joy, K.H. 2012. Basaltic fragments in lunar feldspathic meteorites: connecting sample analyses to orbital remote sensing. *Meteoritics & Planetary Science*, **47**, 387–399, https://doi.org/10.1111/j.1945-5100.2012.01344.x

Robinson, K.L., Barnes, J.J. *et al*. 2016. Water in evolved lunar rocks: evidence for multiple reservoirs. *Geochimica et Cosmochimica Acta*, **188**, 244–260, https://doi.org/10.1016/j.gca.2016.05.030

Sánchez-Lavega, A., Irwin, P. and García Muñoz, A. 2023. Dynamics and clouds in planetary atmospheres from telescopic observations. *The Astronomy and Astrophysics Review*, **31**, 5, https://doi.org/10.1007/s00159-023-00150-9

Satterwhite, C.E. and Righter, K. 2019. *Antarctic Meteorite Newsletter*, **42**. Available online, https://curator.jsc.nasa.gov/antmet/amn/amn.cfm#n422 [last accessed 7 June 2025]

Satterwhite, C.E. and Righter, K. 2020. *Antarctic Meteorite Newsletter*, **43**. Available online, https://curator.jsc.nasa.gov/antmet/amn/amn.cfm#n431 [last accessed 7 June 2025]

Satterwhite, C.E. and Righter, K. 2022. *Antarctic Meteorite Newsletter*, **45**. Available online, https://curator.jsc.nasa.gov/antmet/amn/amn.cfm#n452 [last accessed 7 June 2025]

Schmidt, M.W. and Kraettli, G. 2022. Experimental crystallization of the lunar magma ocean, initial selenotherm and density stratification, and implications for crust formation, overturn and the bulk silicate moon composition. *Journal of Geophysical Research Planets*, **127**, e2022JE007187, https://doi.org/10.1029/2022JE007187

Schneider, C.A., Rasband, W.S. and Eliceiri, K.W. 2012. NIH Image to ImageJ: 25 years of image analysis. *Nature Methods*, **9**, 671–675, https://doi.org/10.1038/nmeth.2089

Schweitzer, A.R., McLeod, C.L. and Shaulis, B. 2022*a*. Geochemical and petrologic insights into a lunar basaltic breccia: Dominion Range (DOM) 18543. 53rd Lunar and Planetary Science Conference, The Woodlands, TX, 7–11 March, abstract #2030, https://www.hou.usra.edu/meetings/lpsc2022/pdf/2030.pdf

Schweitzer, A.R., McLeod, C.L., Shaulis, B. and Loocke, M. 2022*b*. New Petrological insights into a lunar basaltic breccia meteorite from the Dominion Range, Antarctica: DOM 18543. American Geophysical Union Fall Meeting, Chicago, IL, 12–16 December, https://ui.adsabs.harvard.edu/abs/2022AGUFM.P42C2432S/abstract

Shaulis, B.J., Righter, M., Lapen, T.J., Jolliff, B.L. and Irving, A.J. 2017. 3.1 Ga crystallization age for magnesian and ferroan gabbro lithologies in the Northwest Africa 773 clan of lunar meteorites. *Geochimica et*

*Cosmochimica Acta*, **21**, 435–456, https://doi.org/10.1016/j.gca.2017.06.031

Shearer, C.K. and Papike, J.J. 1993. Basaltic magmatism on the Moon: a perspective from volcanic picritic glass beads. *Geochimica et Cosmochimica Acta*, **57**, 4785–4812, https://doi.org/10.1016/0016-7037(93)90200-G

Shearer, C.K., Hess, P.C. *et al*. 2006. Thermal and magmatic evolution of the Moon. *Reviews in Mineralogy and Geochemistry*, **60**, 365–518, https://doi.org/10.2138/rmg.2006.60.4

Shearer, C.K., Elardo, S.M., Petro, N.E., Borg, L.E. and McCubbin, F.M. 2015. Origin of the lunar highlands Mg-suite: an integrated petrology, geochemistry, chronology, and remote sensing perspective. *American Mineralogist*, **100**, 294–325, https://doi.org/10.2138/am-2015-4817

Shearer, C., Neal, C.R. *et al*. 2023. Magmatic evolution II: a new view of post-differentiation magmatism. *Reviews in Mineralogy & Geochemistry*, **89**, 147–206, https://doi.org/10.2138/rmg.2023.89.04

Shen, D., Li, S. *et al*. 2025. Petrogenesis of Chang'E-6 basalts and implication for multi-episode volcanism in the lunar farside basin. *Earth and Planetary Science Letters*, **659**, 119335, https://doi.org/10.1016/j.epsl.2025.119335

Shen, J., Zhang, Y. *et al*. 2024. A pristine low-Ti cumulate source for Chang'e 5 basalts revealed by Sr-Nd-Hf isotopes. *Geochemical Perspectives Letters*, **33**, 44–50, https://doi.org/10.7185/geochemlet.2502

Sheng, S.-Z., Wang, S.-J. *et al*. 2025. Lunar primitive mantle olivine returned by Chang'e-6. *Nature Communications*, **16**, 3759, https://doi.org/10.1038/s41467-025-58820-4

Shih, C.Y., Haskin, L.A., Wiesmann, H., Bansal, B.M. and Brannon, J.C. 1975. On the origin of high-Ti mare basalts. Lunar and Planetary Science Conference Proceedings, Houston, TX, Volume **6**, 1255–1285.

Slyuta, E.N. 2014. Physical and mechanical properties of the lunar soil (a review). *Solar System Research*, **48**, 330–353, https://doi.org/10.1134/S0038094614050050

Slyuta, E. 2021. The Luna program. *In*: Longobardo, A (ed) *Sample Return Missions – The Last Frontier of Solar System Exploration*. Elsevier, 37–78, https://doi.org/10.1016/B978-0-12-818330-4.00003-3

Snape, J.F., Nemchin, A.A., Whitehouse, M.J., Merle, R.E., Hopkinson, T. and Anand, M. 2019. The timing of basaltic volcanism at the Apollo landing sites. *Geochimica et Cosmochimica Acta*, **266**, 29–53, https://doi.org/10.1016/j.gca.2019.07.042

Srivastava, Y., Basu Sarbadhikari, A., Yamaguchi, A., Takenouchi, A., Day, J.M.D. and Ubide, T. 2024. Magmatic evolution of KREEP-free lunar meteorite Asuka-881757 inferred from sector-zoned clinopyroxene, pyroxene symplectites, and thermodynamic modeling. *Meteoritics & Planetary Science*, **59**, 2938–2955, https://doi.org/10.1111/maps.14257

Steenstra, E.A., Agmon, N., Bendy, J., Klemme, S., Mateev, S. and van Westrenen, W. 2018. Depletion of potassium and sodium in mantles of Mars, Moon and Vesta by core formation. *Nature Scientific Reports*, **9**, 7053, https://doi.org/10.1038/s41598-018-25505-6

Stöffler, D. and Grieve, R.A.F. 2007. Impactites. *In*: Fettes, D. and Desmons, J. (eds) *Metamorphic Rocks: A Classification and Glossary of Terms, Recommendations of the International Union of Geological Sciences*. Cambridge University Press.

Stöffler, D., Hamann, C. and Metzler, K. 2018. Shock metamorphism of planetary silicate rocks and sediments: proposal for an updated classification system. *Meteoritics & Planetary Science*, **53**, 5–49, https://doi.org/10.1111/maps.12912

Su, F., Zhang, X. *et al*. 2025. Constraining 2.0 Ga volcanism on the Moon via $^{40}Ar/^{39}Ar$ dating of the Chang'e-5 basalts. *Journal of Geophysical Research: Planets*, **130**, e2024JE008495, https://doi.org/10.1029/2024JE008495

Taylor, G.J. 1994. The scientific legacy of Apollo. *Scientific American*, **271**, 40–47, https://www.jstor.org/stable/24942765 https://doi.org/10.1038/scientificamerican0794-40

Taylor, G.J., Keil, K. and Warner, R.D. 1977. Very low-Ti mare basalts. *Geophysical Research Letters*, **4**, 207–210, https://doi.org/10.1029/GL004i006p00207

Taylor, L.A., Patchen, A., Mayne, R.G. and Taylor, D.-H. 2004. The most reduced rock from the moon, Apollo 14 basalt 14053: its unique features and their origin. *American Mineralogist*, **89**, 1617–1624, https://doi.org/10.2138/am-2004-11-1205

Taylor, S.R. 1992. *Solar System Evolution: a New Perspective*. Cambridge University Press, New York.

Terada, K., Sasaki, Y., Anand, M., Joy, K.H. and Sano, Y. 2007. Uranium–lead systematics of phosphates in lunar basaltic regolith breccia, Meteorite Hills 01210. *Earth and Planetary Science Letters*, **259**, 77–84, https://doi.org/10.1016/j.epsl.2007.04.029

Thalmann, C., Eugster, O., Herzog, G.F., Xue, S., Klein, J., Krähenbühl, U. and Vogt, S. 1996. History of lunar meteorites Queen Alexandra Range 93069, Asuka 881757, and Yamato 793169 based on noble gas isotopic abundances, radionuclide concentrations, and chemical composition. *Meteoritics & Planetary Science*, **31**, 857–868, https://doi.org/10.1111/j.1945-5100.1996.tb02119.x

Tian, H.-C., Yang, W. *et al*. 2023. Reassessing the classification of Chang'e-5 basalts using pyroxene composition. *Lithos*, **456–357**, 107309, https://doi.org/10.1016/j.lithos.2023.107309

Torigoye-Kita, N., Misawa, K., Dalrymple, G.B. and Tatsumoto, M. 1995. Further evidence for a low U/Pb source in the moon: U Th Pb, Sm Nd, and Ar Ar isotopic systematics of lunar meteorite Yamato-793169. *Geochimica et Cosmochimica Acta*, **59**, 2621–2632, https://doi.org/10.1016/0016-7037(95)00154-9

Tosi, N. and Padovan, S. 2021. Mercury, Moon, Mars: surface expressions of mantle convection and interior evolution of stagnant-lid bodies. *In*: Marquardt, H., Ballmer, M., Cottaar, S. and Konter, J. (eds) *Mantle Convection and Surface Expressions*. American Geophysical Union, https://doi.org/10.1002/9781119528609.ch17

Udry, A., Haworth, G.H., Herd, C.D.K., Day, J.M.D., Lapen, T.J. and Filiberto, J. 2020. What martian meteorites reveal about the interior and surface of mars. *Journal of Geophysical Research Planets*, **125**, e2020JE006523, https://doi.org/10.1029/2020JE006523

Udry, A., Ostwald, A.M., Day, J.M.D. and Hallis, L.J. 2025. Fundamental constraints and questions from the study of Martian meteorites and the need for returned samples. *Proceedings of the National Academy of Sciences*, **122**, e2404254121, https://doi.org/10.1073/pnas.2404254121

Wang, K. and Jacobsen, S.B. 2016. Potassium isotopic evidence for a high-energy giant impact origin of the Moon. *Nature*, **538**, 487–490, https://doi.org/10.1038/nature19341

Warren, P.H., Jerde, E.A. and Kallemeyn, G.W. 1989. Lunar meteorites: siderophile element contents, and implications for the composition and origin of the Moon. *Earth and Planetary Science Letters*, **91**, 245–260, https://doi.org/10.1016/0012-821X(89)90001-0

Wiedner, M.C., Aalto, S. *et al*. 2021. Origins space telescope: from first light to life. *Experimental Astronomy*, **51**, 595–624, https://doi.org/10.1007/s10686-021-09782-0

Wood, J.A., Dickey, J.D., Jr, Marvin, U.B. and Powell, B.N. 1970. Lunar anorthosites. *Science*, **167**, 602–604, https://doi.org/10.1126/science.167.3918.602

Yin, C., Chen, J. *et al*. 2025. Petrogenesis of Chang'e-6 basalts and implication for the young volcanism on the lunar farside. *The Astrophysical Journal Letters*, **981**, 1.2, https://doi.org/10.3847/2041-8213/adaf20

Zeigler, R.A., Korotev, R.L., Jolliff, B.J. and Haskin, L.A. 2005. Petrography of lunar meteorite MET 01210, a new basaltic regolith breccia. 36th Lunar and Planetary Science Conference, The Woodlands, TX, 14–18 March, abstract #2385, https://www.lpi.usra.edu/meetings/lpsc2005/pdf/2385.pdf

Zeigler, R.A., Korotev, R.L. and Jolliff, B.L. 2007. Miller Range 05035 and Meteorite Hills 01210: two basaltic lunar meteorites, both likely source-paired with Asuka 881757 and Yamato793169. 38th Lunar and Planetary Science Conference, The Woodlands, TX, 16–20 March, abstract #2110, https://www.lpi.usra.edu/meetings/lpsc2007/pdf/2110.pdf

Zeigler, R.A., Gross, J., Eckley, S. and Vander Kaaden, K.E. 2021. Petrology, geochemistry, and pairing of lunar meteorites from the Dominion Range. 84th Annual Meeting of the Meteoritical Society, 15–21 August, abstract #6141, https://onlinelibrary.wiley.com/doi/pdf/10.1111/maps.13727

Zhang, Q.W.L., Yang, M.H. *et al*. 2024. Lunar farside volcanism 2.8 billion years ago from Chang'e-6 basalts. *Nature*, **643**, 356–360, https://doi.org/10.1038/s41586-024-08382-0

Zhang, Q.W.L., Su, B. *et al*. 2025. Compositional complexity of heterogeneous impact glasses in lunar soils: significance and pitfalls. *Contributions to Mineralogy and Petrology*, **180**, https://doi.org/10.1007/s00410-025-02220-w

Zhou, W.-Y., Olson, P.L. *et al*. 2022. High pressure-temperature phase equilibrium studies on Martian basalts: implications for the failure of plate tectonics on Mars. *Earth and Planetary Science Letters*, **594**, 117751, https://doi.org/10.1016/j.epsl.2022.117751

Ziethe, R., Seiferlin, K. and Hiesinger, H. 2009. Duration and extent of lunar volcanism: comparison of 3D convection models to mare basalt ages. *Planetary and Space Science*, **57**, 784–796, https://doi.org/10.1016/j.pss.2009.02.002